



STUDY REPORT

No. 109 (2001)

Pseudo-dynamic Evaluation of Timber-Framed Walls

S. J. Thurston

The work reported here was jointly funded by Building Research Levy and the Foundation for Research, Science and Technology from the Public Good Science Fund.



© BRANZ 2002

ISSN: 0113-3675

Preface

This report summarises the theory and test work behind the development of a structural pseudo-dynamic testing facility at BRANZ. It includes full description of the analysis to enable verification by others. Future use of the facility is discussed.

Acknowledgments

This work was jointly funded by the Building Research Levy and the Public Good Fund of the Foundation for Research, Science and Technology.

Note

This report is intended for standards committees, structural engineers, architects, designers and others researching earthquake and wind resistance of low-rise buildings.

PSEUDO-DYNAMIC EVALUATION OF TIMBER-FRAMED WALLS

BRANZ Study Report SR 109 (2001)

S. J. Thurston

REFERENCE

Thurston, S.J. 2002. Pseudo-dynamic Evaluation of Timber-Framed Walls. Study Report SR109 (2001). BRANZ, Judgeford, New Zealand.

ABSTRACT

This report describes in detail the development of a pseudo-dynamic structural testing facility for evaluation of timber-framed walls as developed at BRANZ. It covers the theory, the equipment, the software and verification. The benefits and planned use of the pseudo-dynamic testing are described.

Contents

Page No.

1.	Introduction.....	1
2.	Literature Review	2
2.1	Comparison of PD, Shake-table and Computer Model Simulation.....	2
2.2	Numerical Integration Scheme	3
2.3	Level of Damping to Use in PD Analysis	3
2.4	Full House-Shaking Test in USA.....	4
3.	Advantages and Disadvantages of the PD Test Method.....	4
4.	Types of PD Tests Currently Programmed.....	5
5.	Damping in single degree of Freedom Systems	7
6.	Damping in Multi Degree of Freedom Systems	10
7.	Pseudo-Dynamic Programming Equations and Theory	10
7.1	SDOF Wall.....	10
7.2	2DOF System – not separated	12
7.3	2DOF System – separated	13
7.4	Torsional Response of a Simplified Non-symmetric House	14
7.5	2DOF Torsion System With Perpendicular Walls of Same Properties.....	17
8.	Verification of Program by SDOF Tests	18
8.1	Results	19
8.2	Description of Damage	22
8.3	Conclusions	23
9.	Verification of Program by Two Degrees of Freedom Tests	30
9.1	Construction.....	30
9.2	Results	31
9.3	Sensitivity Analysis.....	31
9.4	Conclusions from ITHA and PD Tests	32
10.	Verification of Program by Torsion Tests	43
10.1	Construction.....	43
10.2	Results	43
10.3	Conclusions	43
11.	Comparison of Ruaumoko, Excel and PD Theoretical Analyses	44
12.	Conclusions.....	45
13.	References.....	45
14.	Acknowledgements.....	46

Appendices

Appendix A	Modified El Centro Earthquake.....	47
------------	------------------------------------	----

Figures

Page No.

Figure 1 : Sketch of Structures Analysed.....	6
Figure 2: Displacement Versus Time Plot From a Typical Free Vibration Test	8
Figure 3: Backbone Load Deflection Plot of a Timber-Framed Lined Wall	8
Figure 4: Surmised Relationship Between House and Element Force/Deflection Relationship	9
Figure 5: Equations of Motion for Constant Slope Acceleration.....	12
Figure 6: Sketch Illustrating the Difference Between a Separated and Non-Separated Two-storey PD Test	14
Figure 7: Analysis Theory - House Torsional Response.....	16
Figure 8: Wall W1. Cyclic Test and Ruaumoko Modelled Hysteresis Loops	19
Figure 9: Wall W2. Cyclic Test and Ruaumoko Modelled Hysteresis Loops	20
Figure 10: Wall W3. Cyclic Test and Ruaumoko Modelled Hysteresis Loops	20
Figure 11: Wall W4. Cyclic Test and Ruaumoko Modelled Hysteresis Loops	21
Figure 12: Deflections Computed Using Different Levels of Damping	21
Figure 13: Wall W1. PD Test and ITHA Hysteresis Loops.....	24
Figure 14: Wall W2. PD Test and ITHA Hysteresis Loops.....	24
Figure 15: Wall W3. PD Test and ITHA Hysteresis Loops.....	25
Figure 16: Wall W4. PD Test and ITHA Hysteresis Loops.....	25
Figure 17: Comparison Ruaumoko and PD. Wall W1, 0.5 El Centro EQ	26
Figure 18: Comparison Ruaumoko and PD. Wall W1, 1.0 El Centro EQ	26
Figure 19: Comparison Ruaumoko and PD. Wall W1, 1.25 El Centro EQ	27
Figure 20: Comparison Ruaumoko and PD. Wall W2, 0.5 El Centro EQ	27
Figure 21: Comparison Ruaumoko and PD. Wall W2, 1.0 El Centro EQ	28
Figure 22: Comparison Ruaumoko and PD. Wall W3, 0.5 El Centro EQ	28
Figure 23: Comparison Ruaumoko and PD. Wall W3, 1.0 El Centro EQ	29
Figure 24: Comparison Ruaumoko and PD. Wall W4, 1.0 El Centro EQ	29
Figure 25: Comparison Ruaumoko and PD. Wall W4, 1.5 El Centro EQ	30
Figure 26: Wall W6. Cyclic Test and Ruaumoko Modelled Hysteresis Loops	33
Figure 27: Wall W5. Cyclic Test and Ruaumoko Modelled Hysteresis Loops	33
Figure 28: Wall W7. PD Test and Ruaumoko Modelled Hysteresis Loops	34
Figure 29: Comparison Ruaumoko and PD. WallSet A, 1.0 El Centro EQ.....	35
Figure 30: Comparison Ruaumoko and PD. WallSet A, 1.5 El Centro EQ.....	36
Figure 31: Comparison Ruaumoko and PD. WallSet B, 1.0 El Centro EQ	37
Figure 32: Comparison Ruaumoko and PD. WallSet E, 1.0 El Centro EQ	38
Figure 33: Sensitivity Analysis WallSet B, 1.0 El Centro EQ.....	39
Figure 34: Comparison Ruaumoko and PD. WallSet C, 1.0 El Centro EQ	40
Figure 35: Comparison Ruaumoko and PD. WallSet C, 1.3 El Centro EQ	41
Figure 36: Comparison Ruaumoko and PD. WallSet D, 1.0 El Centro EQ.....	42
Figure 37: Comparison of the NZS4203 [17] and Modified El Centro response spectrum.....	47
Figure 38: Modified El Centro Earthquake Acceleration Record.....	47

Tables

Page No.

Table 1: Single Walls Tested 18

Table 2: Comparison of Deflections Measured in PD Testing and
Ruaumoko Simulation of SDOF Walls..... 23

Table 3: Two-storey Walls PD- Tested as Separated Walls 30

Table 4: Two-storey Walls PD- Tested as Separated Walls 31

Table 5: Comparison of Deflections Measured in PD Testing and
Ruaumoko Simulation of 2DOF Walls 32

Table 6: Comparison of Deflections Measured in PD Testing and
Ruaumoko Simulation of Torsion Configuration Walls 43

Table 7: Summary of Structures Analysed 44

1. INTRODUCTION

The pseudo-dynamic method was first described in 1974 [1]. This report describes in detail the pseudo-dynamic (PD) structural testing facilities developed at BRANZ. It covers the theory, the equipment, the software and verification, the benefits and the planned use of the PD testing facilities.

The PD test method is a combination of a conventional cyclic test and analytical modelling. The displacements imposed on a test specimen are determined by a computer during the test, based on the measured specimen resistance at each time step, the analytically calculated inertia and damping forces, and the digitised earthquake acceleration record. The displacement histories imposed closely resemble those that would occur if the structure were tested dynamically, such as on a shake-table. It has the advantage over total analytical modelling in that the computations at each instance are based on the measured resistance and the uncertainties associated in calculating this force after a specific deflection time history are not present in a PD test. Faster modern computers and software have largely overcome the speed limitations of the earlier PD programs. BRANZ used National Instruments Corporation LabView Version 6 software [2] on a computer with a clock speed of 800 MHz.

Whereas the seismic mass must be present in a shake-table test, it is simulated in a PD test. The damping in a shake-table test is that which is actually present in the test specimen, whereas again it is simulated in a PD test. These differences lead to many advantages, and some disadvantages as discussed in Section 3. One of the major differences is that the PD test can be performed at a slower rate (say 1/16 real time speed). This provides greater opportunity for viewing the test. However, greater loading speed usually results in slightly greater specimen strength and in this regard the PD test results are expected to be conservative.

A PD test consists of a test specimen with one or more servo-controlled actuators used to apply loads at specific locations. For instance, a multi-storey wall specimen would normally use actuators at each floor level. At the end of each time step, applied forces and specimen deflections are recorded by a computer and, based on these values, the deflections to be imposed during the next time step are calculated. Provided the time step is adequately small, and the measurements are of sufficient accuracy, then this report found good agreement between PD tests and Inelastic Time History Analyses (ITHA).

To verify the PD software and test results, this report presents comparisons of PD test results, with (1) an established ITHA software package known as Ruaumoko [3], and (2) Excel spreadsheet analysis developed by the writer. The good agreement between these three methods gives confidence in all. The agreement between shake-table tests and non-linear dynamic analysis software by others has also been good, as discussed in Section 2. Hence, where a structure can be adequately modelled, then ITHA software can be used to predict the seismic performance.

The seismic performance of houses is usually greatly enhanced by load sharing and composite action of both the structural and non-structural elements and the lateral restraint due to gravity load resisting wall 'rocking action'. Thurston and Park [4] showed that it was necessary to consider this enhanced stiffness and strength (hereafter

called “systems effects”), to avoid undue conservatism when designing to the bracing wall provisions in the New Zealand Standard for Timber Framed Buildings NZS3604:1999 [5]. These influences are difficult to model and are discussed further in Section 2. Shake-table tests of total houses require very large shake-tables and rely on the fidelity of the applied ground accelerations.

Most New Zealand houses are designed and constructed using the non-specific design procedures in NZS 3604:1999. The PD facilities have been developed to enable BRANZ to measure seismic performance of New Zealand houses and to verify software analysis methods. The results will be used to check that current NZS 3604 requirements are adequate to ensure good seismic performance of New Zealand houses and to propose modifications if required.

2. LITERATURE REVIEW

2.1 Comparison of PD, Shake-table and Computer Model Simulation

Mahin [6] reported on a total of 13 PD tests by four research centres around the world. Those on one-storey and two-storey steel and reinforced concrete structures gave good agreement with equivalent analytical and shake-table tests. Those on a six-storey braced steel frame and a seven-storey reinforced concrete building indicated the practicality of the method but highlighted the need for more research to improve its reliability for multi-storey structures. Mahin himself verified the PD method for single degree of freedom systems by correlating PD tests with shake-table and analytical simulations. He noted that difficulties can be expected in accurately PD testing stiff systems with large degrees of freedom that are sensitive to experimental errors. To overcome this, Seible et al [7] conducted a PD test using the response of the top storey only. The actuators applied a fixed proportion of the force at the lower two levels of his three-storey structure.

Kamiya [8] performed pseudo-dynamic tests using simulated seismic loading on six plywood shearwalls of different construction. He developed a computer model of the cyclic hysteresis loops based on measured test parameters of full-scale walls. The theoretical load and displacements were within 5% of the pseudo-dynamic test results. Kamiya assumed 10% damping for both types of analyses.

Ceccotti et al [9] performed a cyclic racking test on a wall element and a pinching model was matched to test data. The wall element was then tested on a shake-table by Tsukuba. ITHA software called Drain2d with the Ceccotti element was used to simulate the racking test. Agreement was good.

Under task 1.1.1 of the CUREe-Caltech Wood-frame Project [10], a typical USA construction two-storey wood-frame house was tested under unidirectional shake-table imposed simulated seismic loading. Measured damping was 7.6%. The authors of the report used ITHA (using the Ruaumoko [3] software with the Stewart [11] hysteresis model and 7.6% damping) to predict the response of the walls. The Stewart [11] model was based on the Cashew [12] computer program prediction of the wall load versus deflection cyclic hysteresis loops. The ITHA over-predicted displacements at low levels of shaking by factors of approximately two and gave a natural frequency approximately 30% less than measured. However, agreement was good at high levels of shaking. The

discrepancy at low levels of damping was attributed to the initial stiffness modelled for the walls being less than that in the test structure.

Deam and King [13] developed a continuous pseudo-dynamic system using an analogue integration scheme in an attempt to avoid a “stop-go” movement of the test specimen. However, the advent of faster computers and software described in this report has meant that timesteps are so small that progress of the test is effectively continuous.

In summary, these papers indicate good agreement between shake-table, computer model and PD testing.

2.2 Numerical Integration Scheme

Mahin [6] proposed using the Explicit Newmark method for numerical integration with $\beta = 0$ and $\gamma = 0.5$ which effectively assumes a constant acceleration over the following time step. The writer found greater accuracy of computation, and greater ease to extend the method to multi-degree of freedom systems, if the assumption is made that there is the same linear change in acceleration in the next time step as in the last. The mathematics are given in Figure 5. This assumption enables the velocities and displacements at timestep t_{n+1} to be calculated if the accelerations, velocities and displacements at timestep t_n are known. Thus, the accelerations can then be calculated from the force balance equations (see Eqn. 5) and the solution can proceed. Other variations of the integration scheme are discussed by Deam et al [13].

2.3 Level of Damping to Use in PD Analysis

The level of damping to use in a PD analysis must be assumed and, ideally, should be based on free vibration tests of the complete structure. It cannot be reliably based on free vibration tests on a substructure unless the full mass and non-structural elements are present. It is important that the initial stiffness taken to calculate the damping from the percentage of critical damping measured is the same as assumed in the computer analysis and/or PD test. This is discussed in more detail in Section 5. The literature shows a wide scatter of damping measured or assumed and this may be partially due to the initial stiffness assumed/used as discussed in Section 5.

Kamiya [8] used 10% damping for pseudo-dynamic tests using simulated seismic loading on six plywood shearwalls of different construction. He developed a computer model of the cyclic hysteresis loops based on measured test parameters of full-scale walls. The theoretical load and displacements were within 5% of the pseudo-dynamic test results.

Shaking table tests were performed by Yamaguchi et al [14] on a box-like structure incorporating full-scale house walls. The main resisting elements were plywood walls. The nails tended to pull out of these walls and peak load reductions of over 50% were experienced. They found their shake-table tests were best modelled with an assumed 2% damping. However, data given to support this was sparse. Compared with the slow cyclic tests their shake-table test specimens exhibited greater strength but lower ductility.

Houses with plasterboard walls were found to have a natural period of 0.16 seconds by Kohara et al [15]. At a deflection of 20 mm, the damage was limited to buckling of the braces, cracking in the plasterboard and material damage at nail heads in both the plywood and plasterboard walls. This appeared to be simply repairable and non-life threatening.

2.4 Full House-Shaking Test in USA

Under task 1.1.1 of the CUREe-Caltech Woodframe Project [10], a two-storey woodframe house was tested under simulated seismic loading using two 1994 Northridge earthquake motions. The exterior walls, lined with oriented strand board (OSB) structural panels, were intended as the main load-resisting element. The roof deflections reached depended on the phase of the project but exceeded 50 mm in phase 6. Damage was generally small and isolated to the OSB nailed connections. The diaphragm to shear wall deflection was generally less than 20% which implies a classification of rigid. Lining the house with gypsum plasterboard approximately doubled the house natural frequency and reduced the deflections by a factor of three.

The building damping was determined from free vibration decay curves. There was significant scatter in the results but an average value of 7.6% was obtained. The authors used THIA software (Ruaumoko [3] with the Stewart [11] hysteresis model) to predict the response of the walls.

As expected, addition of plasterboard lining almost doubled the structure's natural frequency. After each set of tests there was a drop in the natural frequency. Non-symmetrical openings caused a significant torsional response of the structure.

Uplift forces were greater than predicted and the uplift deflections were significant – reaching up to 20 mm during high shaking. This was surprising when the end studs were fairly rigidly held down.

The authors provide an excellent summary of full-scale house testing done to date.

3. ADVANTAGES AND DISADVANTAGES OF THE PD TEST METHOD

PD tests are performed at a slower speed than real time. This ensures that actual damping and acceleration forces are negligible and can be ignored in a force balance at a particular node in a PD test. This enables the measured forces to be used directly in the equations of motion. The mathematics for this are given in Section 7.1. However, this results in two disadvantages relative to shake-table tests:

1. The slower speed does not model the enhanced strength often present in dynamic tests due to high rate of loading when compared to slow cyclic tests.
2. The damping must be simulated rather than using the actual damping present in the test specimen. (This damping can be obtained by separate tests such as from free vibration following an initial offset.) However, on the positive side, and if desired, greater damping may be used in a PD test than present in the test specimen to account for non-structural damping effects.

There are significant advantages in the PD test method relative to the shake-table tests.

1. The main advantage is that the shake-table and large seismic mass are not required. The tables for large constructions are expensive and the fidelity of the earthquake motion induced is often poor. The large seismic mass must generally be supported at the top of the specimen and be able to move free laterally while being separately supported vertically. Consequently, larger specimens can be tested in PD tests.
2. The specimen may be tested so that it responds as though it is within a complete structure because the remainder of the test specimen can be modelled analytically.
3. As shown in Section 7.3, PD tests can be used for multi-storey substructures tested as a series of single-storey constructions, provided the vertical loads from seismic action are not consequential or are carried by other parts of the main structure. For instance, a beam under a top-storey floor may carry the seismic vertical forces to columns rather than being carried by the shear wall in the floor below. This is a construction saving.
4. Also, as shown in Sections 7.4 and 7.5, PD tests can be used for single-storey torsional investigations using just two walls and assuming a rigid diaphragm. This is a construction saving.
5. It is easier to observe specimen behaviour and measure specimen deflection.
6. The shear force distribution within the test specimen can be obtained directly from the measured forces. Thus, element and specimen load versus deflection hysteresis loops are an automatic bi-product of the PD test. This is more difficult to achieve from the results of a shake-table test.

4. TYPES OF PD TESTS CURRENTLY PROGRAMMED

This report discusses the development of the BRANZ PD testing facility for evaluation of five different types of structure:

- (1) Single-storey wall or building without torsional effects. (See Figure 1(a)).
- (2) Two-storey wall or building without torsional effects. (See Figure 1 (b)).
- (3) Two-storey wall or building without torsional effects but constructed as two single-storey structures (each similar to Figure 1(a)). The interaction between the two structures is simulated. This is called “Separated Construction”.
- (4) Single-storey building consisting of four walls at designated positions and a rigid ceiling diaphragm. (See Figure 1 (c)). The walls are assumed to be the summations of half the walls of the house in that direction. Two actuators apply forces along the lines of two walls as shown. These are the two test walls and in this study Wall W1 was made significantly less stiff and of lower yield strength than Wall W2 to make the structure sensitive to torsion. The perpendicular walls (Wall W3 and Wall W4) are used to resist floor rotation. However, in this analysis Wall W3 and Wall W4 are simulated as elastic walls and thus become more effective at resisting floor rotation after yielding reduces the stiffness of Wall W1 and Wall W2.

- (5) Single-storey building symmetrical about an axis through points P and R; (i.e. the structure in Figure 1(c) is taken to have Wall W3 identical to Wall W1 and Wall W2 identical to Wall W4). All walls are taken to be inelastic which intuitively will result in a greater sensitivity to torsion. The earthquake direction is along line QS which is at 45° to the house main axes to maximise torsion effects. The symmetry allows the system to be decoupled to just Wall W1 and Wall W2 acted upon by an X direction earthquake through the centre of mass with earthquake magnitude reduced by $\sqrt{2}$.

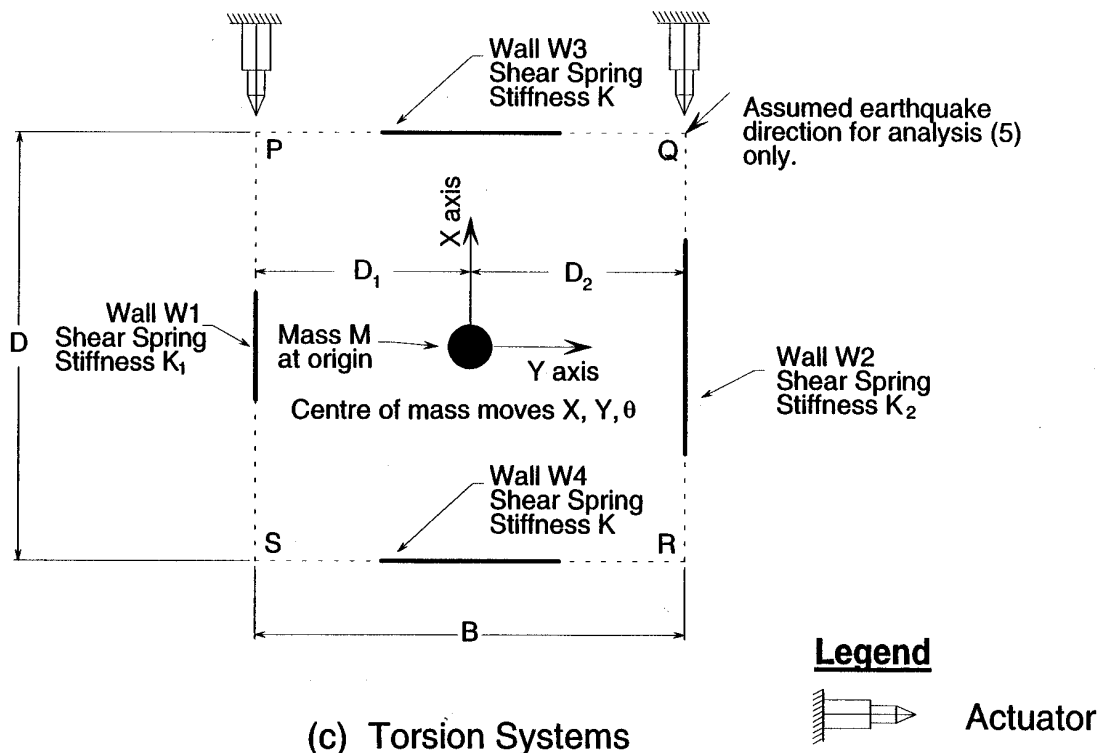
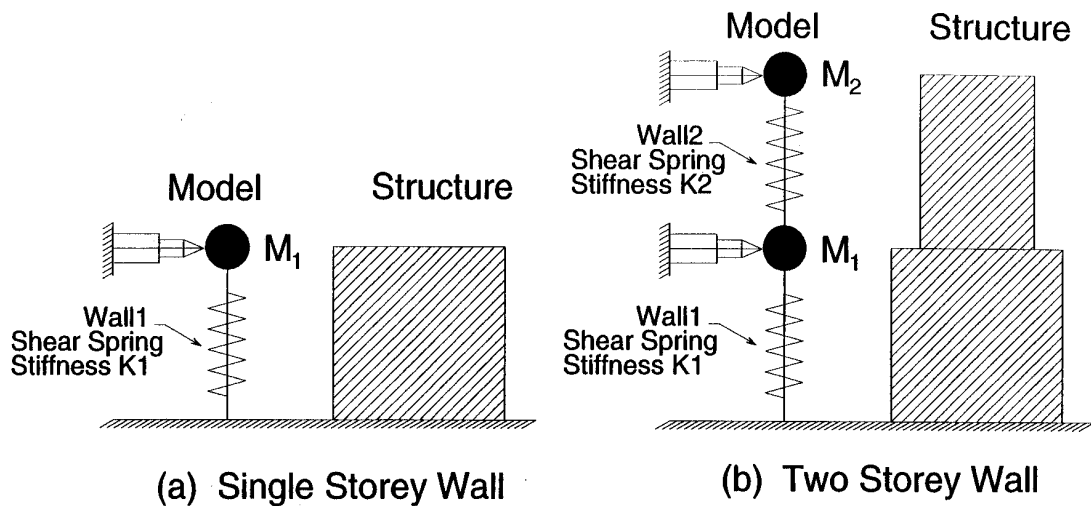


Figure 1 : Sketch of Structures Analysed

For each of the above structural forms various types of analysis are available:

- (a) Actual PD test where a specimen is displaced under simulated seismic motion. At each time step the program sends instructions to move the actuators to designated locations and then measures the forces that were applied to the specimen at the end of the time step. This data is then used in the computations of displacement for the next time step.
- (b) Instead of measuring the forces the program can be asked to calculate the forces based purely on the command deflection. The calculated forces are either command deflections factored by specified stiffnesses or else as calculated, assuming that the specimen behaviour is bilinear. Thus the LabView program acts as a stand-alone theoretical software analysis package and the output can be directly compared with other software analysis packages. The purpose of this LabView program alternative theoretical analysis is purely to verify the algorithms used in common with the PD test to give assurance of its reliability. Results are presented in Appendix A as comparisons of the LabView theoretical analysis with those from other software analysis packages.
- (c) At each time step the program sends instructions to move the actuators to designated locations but the forces are calculated from the measured actuator deflections factored by specified stiffnesses. Using this facility, the actuators can then be observed making realistic motions. This should be used prior to any PD test to help ensure that the electronics are correctly connected, the selected excitation is appropriate and the hydraulic ram control electronics are set up properly. We have found that undertaking this step avoids set-up problems which otherwise would have resulted in the test specimen being destroyed in an incorrectly performed PD test.

For each of the above analysis and structural forms, the input can be specified as one of a selection of earthquakes, a pulse of given magnitude and time, or a continuous Sinusoidal excitation.

5. DAMPING IN SINGLE DEGREE OF FREEDOM SYSTEMS

Consider the forces on a single degree of freedom (SDOF) wall subjected to a ground acceleration \ddot{G}_x (as shown in Figure 1a). The seismic mass at the top of the wall of elastic stiffness K is taken to be M and the deflection at the top of the wall is taken to be X . A force balance at the mass provides the following equation:

$$M \ddot{X} + C \dot{X} + KX = -M \ddot{G}_x$$

The stiffness K is a function of X in non-linear systems.

The term C is the damping restoring force per unit velocity. Chopra [16] stated that this is not well understood but is thought to be the cumulative friction (parts rubbing together) including air resistance to motion. It is separate from hysteretic damping which is the energy absorbed by the inelastic action of the structural element. Hysteretic damping is effectively simulated from the shape of the hysteresis loop used in the analysis.

Damping is usually expressed in terms of the ratio of critical damping, I , and for a SDOF structure it can be shown [16] that:

$$C = 2I\sqrt{K.M} \dots\dots(1)$$

For elastic systems the ratio of critical damping, I , can be determined from the ratio of peaks in free vibration decay curves (see Figure 2 using eqn (2)). The New Zealand Loadings Standard, NZS4203:1992 [17] assumes $I = 5\%$ for bilinear systems (e.g. steel) are effectively elastic below first yield and thus calculating C assuming a constant K from eqn. (1) appears to be reasonable. However, house wall systems exhibit non-linearity from the outset and this makes determination of I questionable, as discussed below.

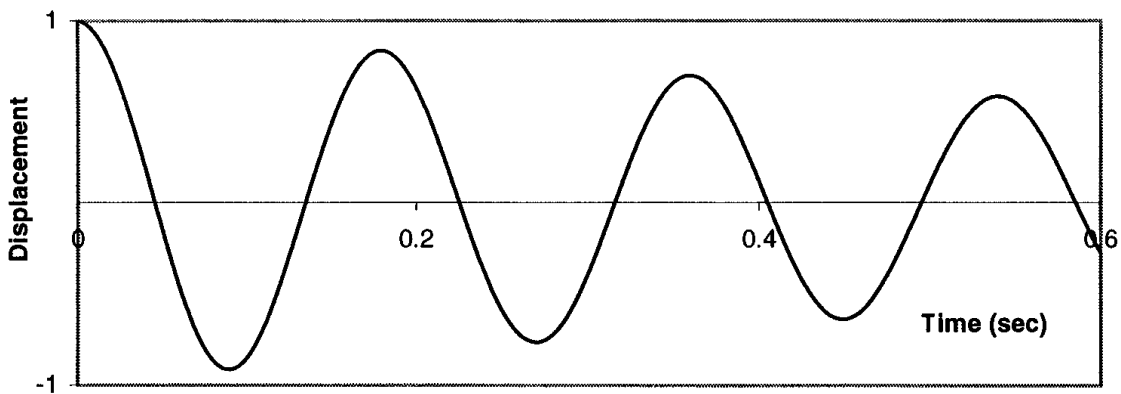


Figure 2: Displacement Versus Time Plot From a Typical Free Vibration Test

The inherent ratio of critical damping (λ) in a freely vibrating system can be determined from the ratio, R , of the $(i)^{th}$ and $(i+j)^{th}$ peaks of either displacement or acceleration. Damping is found using the expression [16]:

$$\frac{I}{\sqrt{1-I^2}} = \frac{1}{2pj} \ln R. \quad \text{For small } I (<0.3), \quad I = \frac{1}{2pj} \ln R \quad \dots\dots(2)$$

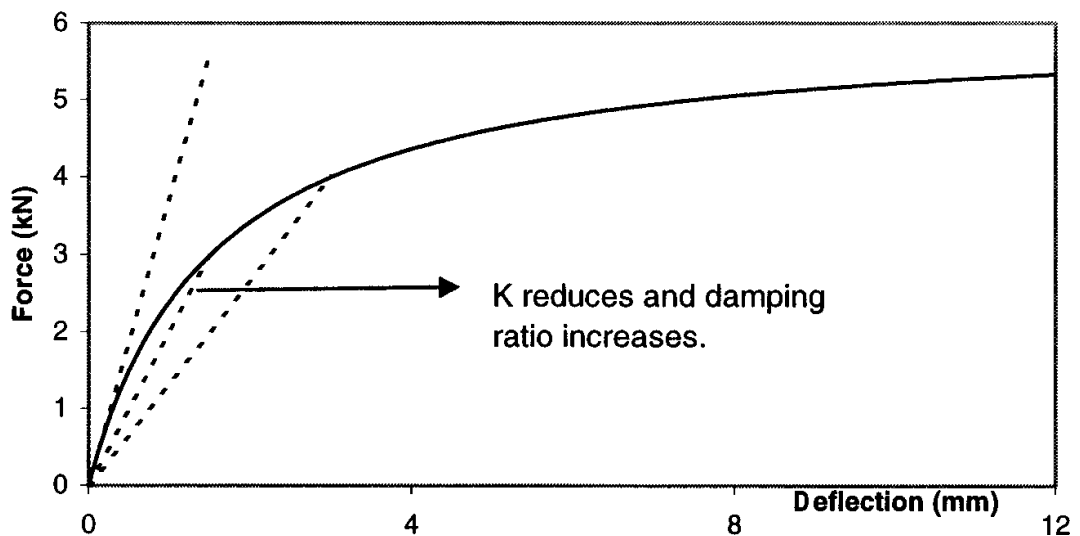


Figure 3: Backbone Load Deflection Plot of a Timber-Framed Lined Wall

For an inelastic system with the initial load deflection curve being non-linear, repeat cycles to the same small deflection may give close to an elastic response. However, for many wall linings the stiffness K will be a function of the selected small deflection as illustrated in Figure 3. Thus, the ratio of critical damping so determined

$$(I = \frac{C}{2\sqrt{K.M}})$$

will vary as a function of the selected small deflection as C is largely independent of the deflection. This does not appear to be well understood by researchers who measure damping ratio, I , from free vibrations tests [16] but who do not provide the deflection limit at which it was measured. Some researchers subsequently do a shake-table test on the element and run a non-linear computer simulation for comparison. However, the initial stiffness of the element in the computer simulation does not correspond to the deflection at which the twanging tests were performed, which means that the actual damping C in the computer simulation is incorrect.

If free vibration tests are performed on timber-framed shear walls at very low displacements then low values of I will be derived as K is high. However, if the tests are done at displacements at which non-linearity is significant, then the damping will also contain a hysteretic component and values of I derived will be too high.

It is difficult to determine appropriate levels of damping in full-house testing where non-structural elements give a house a high initial stiffness, and thus values of I derived from the free vibration tests are low. However, in non-linear computer analysis of the house behaviour only structural elements are included and the model thus has a significantly lower initial stiffness than the house, and hence the value of C used will be too low if it is based on the house free vibration testing.

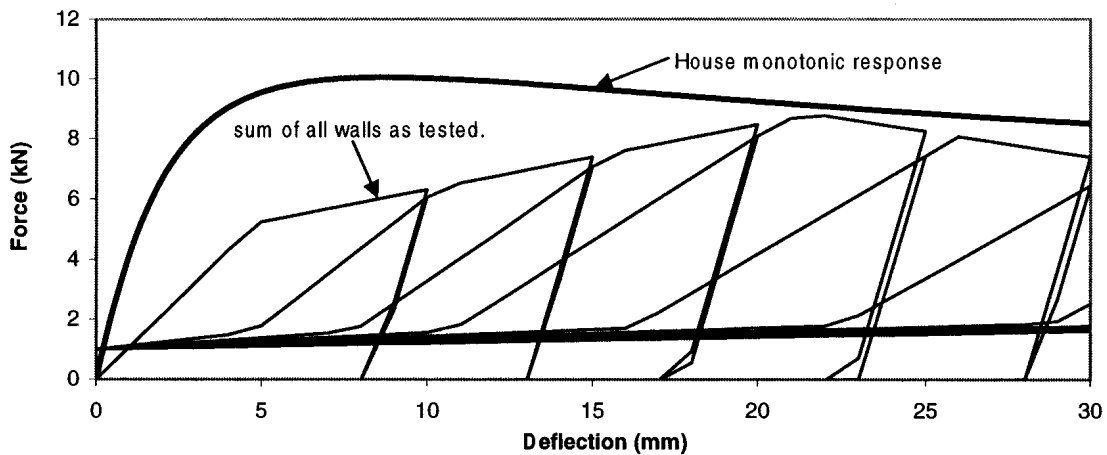


Figure 4: Surmised Relationship Between House and Element Force/Deflection Relationship

The expected relationship between the full-house monotonic load deflection relationship and the first quadrant of the cyclic hysteresis loops for the sum of all structural walls (as determined from tests on separate walls) is shown in Figure 4. The house is expected to be significantly stiffer, reach a higher resistance and perhaps reach peak load at a smaller deflection. If the house damping obtained from a small displacement twanging test was 8% and if the house had an initial stiffness of twice that of the separated

structural walls then the damping to be used in an ITHA model with loops as expected from summing separated walls should be increased to $8\sqrt{\frac{K_{TEST}}{K_{MODEL}}} = 8*\sqrt{2} = 11.3\%$.

6. DAMPING IN MULTI DEGREE OF FREEDOM SYSTEMS

The damping used in this report is the Rayleigh initial stiffness damping (sometimes called proportional damping). The description given below is from Carr [3]. Carr also outlined various other damping models.

The damping forces are assumed to be a factor of the damping matrix [C] and the matrix of the velocity $\left\{ \dot{u} \right\}$ as shown in eqn (5). In the Rayleigh method, the matrix [C] is obtained from the mass matrix [M] and the stiffness matrix [K] using:

$$[C] = \alpha[M] + \beta[K] \dots\dots\dots(3)$$

$$\text{Where } \alpha = \frac{2.w_i.w_j.(w_i.I_j - w_j.I_i)}{w_i^2 - w_j^2} \text{ and } \beta = \frac{2.(w_i.I_i - w_j.I_j)}{w_i^2 - w_j^2} \dots\dots\dots(4)$$

I_i and I_j are damping ratios for modes i,j with natural frequencies w_i and w_j respectively.

7. PSEUDO-DYNAMIC PROGRAMMING EQUATIONS AND THEORY

From a force balance, Chopra [16] gave the matrix form of the generalised equations of motion of an elastic structure subjected to earthquake excitation:

$$[M] \left\{ \ddot{u} \right\} + [C] \left\{ \dot{u} \right\} + [K] \left\{ u \right\} = - [M] \left\{ \ddot{G} \right\} \dots\dots\dots(5)$$

where u, \dot{u}, \ddot{u} represents the displacement, velocity and acceleration respectively, [M] is the matrix of the inertia of the masses, [C] is the damping matrix, [K] is the stiffness matrix and [G] is the ground motion.

7.1 SDOF Wall

The structure to be analysed under earthquake excitation is shown in Figure 1(a).

A PD test proceeds in a stepwise manner under a step-by-step integration procedure. In each step, the computed displacements are quasi-statically imposed on the test specimen by means of computer controlled electro-hydraulic actuators. The forces applied to the specimen by the actuator as measured at the end of the time step are then used to compute the displacement response in the next step, based on analytically prescribed values of mass, damping and ground acceleration. This process is repeated for the entire earthquake record.

The equations derived here are for an earthquake acceleration applied over a small time step. During this time step the load-deflection relationship for the wall is considered to be perfectly elastic. At the end of the time increment the wall stiffness is reassessed. Thus the methodology can be applied to non-linear systems.

When the seismic mass at the top of the wall is taken to be M , the momentary elastic stiffness K and the deflection at the top of the wall is taken to be X , then Eqn.(5) reduces to:

$$M \ddot{X} + C \dot{X} + KX = -M \ddot{G} \dots\dots(6)$$

A PD test is run at a slower rate than real time (generally PD Time/Real Time >10). Thus, the accelerations and velocities experienced in a PD test are low. Therefore, the inertia and viscous forces can be taken to be zero. Hence, in a PD test, the applied force $F = \text{spring force } (K.X)$ where the convention is X is measured in the direction away from the actuator and a compression force in the actuator is positive. Thus:

$$\ddot{X} = -(C \dot{X} + F + M \ddot{G}) \dots\dots(7)$$

The damping, C , can be found from Equations (3) and (4).

Put $w_j = 0$ and $w_i = \sqrt{\frac{K}{M}}$ and it then follows that $\alpha = 0.$, $\beta = 2I\sqrt{\frac{K}{M}}$, and $C = 2I\sqrt{K.M}$

Hence, if all values on the right hand side of Eqn (7) are known at time T , then \ddot{X} can be calculated. By integrating over the next time step \dot{X} and X at the end of the time step can be calculated. The computer controlling the PD process then sends a signal to make the actuator move the top of the wall to the new calculated X displacement. When this movement is completed at the end of the time step then the applied force F is measured. Therefore, all the information assumed known at time T is now known at time $T+\Delta T$ and so the process can continue.

Many integration processes are available [3]. Each has its own problems and advantages. The simplest is to assume the acceleration is constant over each time step. The time step needs to be small to obtain accuracy. A larger time step may be used if the acceleration slope over the one time increment is assumed to be equal to that of the preceding time increment. The mathematics to calculate the velocity and deflection at the end of the time increment are given in Figure 5 and have been simply obtained by single and double integration of the assumed accelerations.

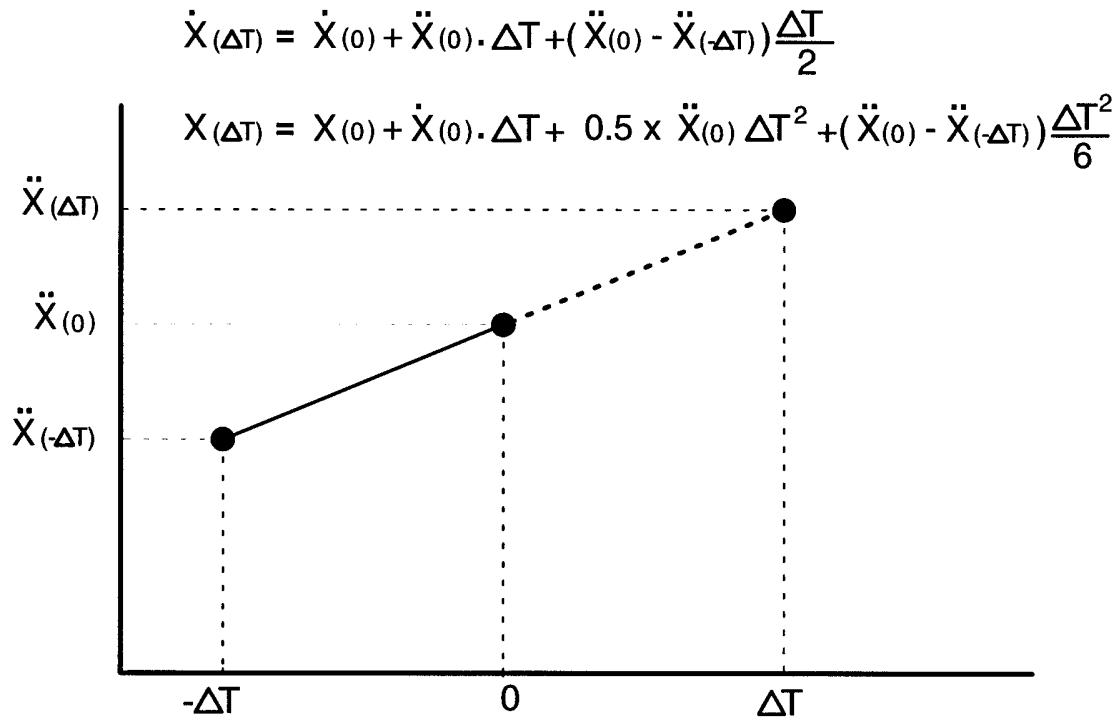


Figure 5: Equations of Motion for Constant Slope Acceleration

7.2 2DOF System – not separated

The structure to be analysed under earthquake excitation is shown in Figure 1(b).

The structure is a two-storey shear wall. The bottom storey (Wall W1) is of elastic stiffness K_1 and the top storey (Wall W2) is of elastic stiffness K_2 . The floor seismic masses are M_1 at Level 1 and M_2 at Level 2. The wall deflections are X_1 and X_2 at Level 1 and 2 respectively. Chopra [16] gives the mass and stiffness matrices as:

$$[M] = \begin{bmatrix} M_1 & 0 \\ 0 & M_2 \end{bmatrix} ; [K] = \begin{bmatrix} K_1 + K_2 & -K_2 \\ -K_2 & K_2 \end{bmatrix}$$

Note, the stiffness coefficient K_{ij} is the force at node i when a unit displacement is given at node j with all other nodes fixed.

The damping coefficients, C_{ij} , can be found from Equations (3) and (4). Namely:

$$C_{11} = \alpha \cdot M_1 + \beta \cdot (K_1 + K_2)$$

$$C_{12} = -\beta \cdot K_2$$

$$C_{21} = -\beta \cdot K_2$$

$$C_{22} = \alpha \cdot M_2 + \beta \cdot K_2$$

Hence, for an earthquake \ddot{G}_x in the direction X of the Wall W1 and Wall W2, eqn. (5) reduces to:

$$\text{At mass } M_1: M_1 \cdot \ddot{X}_1 + C_{11} \cdot \dot{X}_1 + C_{12} \dot{X}_2 + K_1 \cdot X_1 - K_2 \cdot (X_2 - X_1) = -M_1 \cdot \ddot{G}_x \quad \dots(8)$$

At mass M2: $M_2 \cdot \ddot{X}_2 + C_{21} \cdot \dot{X}_1 + C_{22} \dot{X}_2 + K_2 \cdot (X_2 - X_1) = -M_2 \cdot \ddot{G}_x \dots\dots(9)$

In a PD test, (PD time) where the accelerations and velocities are low, the inertia and viscous terms can be taken to be zero. If the force applied by the actuator at Level 1 is F_1 and the force applied by the actuator at Level 2 is F_2 then a force balance at the masses provides the following equations:

At Level 1: $K_1 \cdot X_1 = F_1 + F_2$. At Level 2: $K_2 \cdot (X_2 - X_1) = F_2$. Thus, $F_1 = K_1 \cdot X_1 - K_2 \cdot (X_2 - X_1)$
Hence, equations (8) and (9) reduce to:

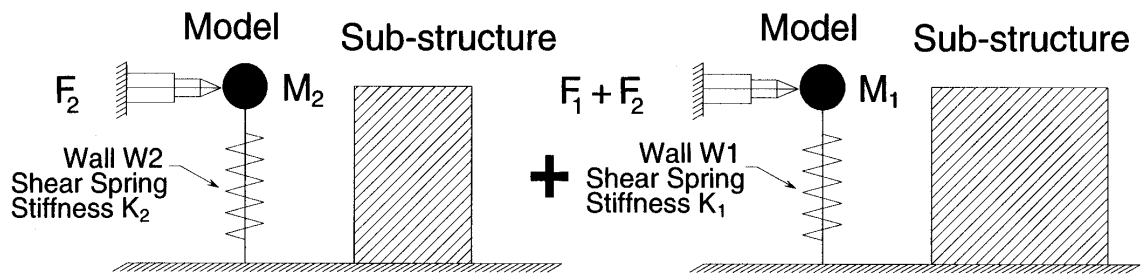
At mass M1: $M_1 \cdot \ddot{X}_1 = -((C_{11} \cdot \dot{X}_1 + C_{12} \dot{X}_2 + F_1) / M_1 + \ddot{G}_x) \dots\dots (10)$

At mass M2: $M_2 \cdot \ddot{X}_2 = -((C_{21} \cdot \dot{X}_1 + C_{22} \dot{X}_2 + F_2) / M_2 + \ddot{G}_x) \dots\dots (11)$

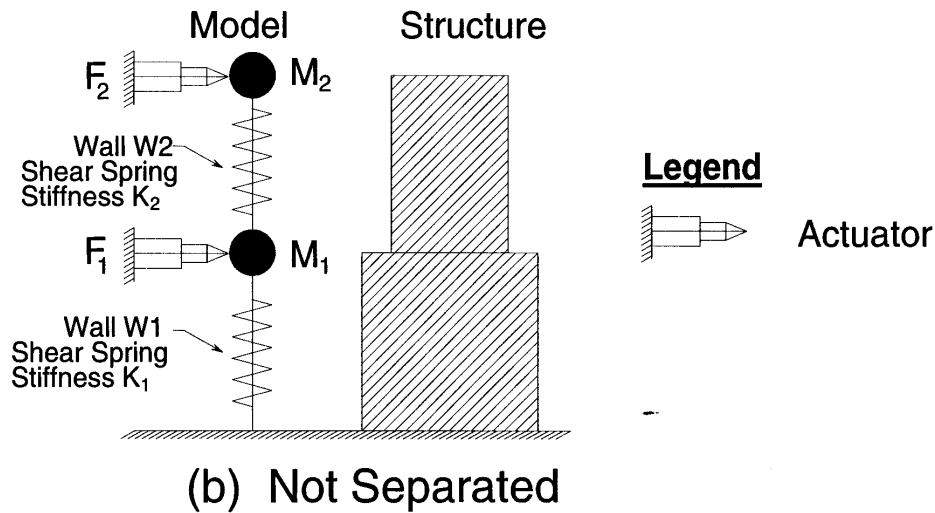
Therefore, if all values on the right hand side of Eqns (10) and (11) are known at time T, then \ddot{X}_1 and \ddot{X}_2 can be calculated. By integrating over the next time step, the velocities and displacements at X_1 and X_2 can be calculated. The computer controlling the PD process then sends a signal to make the actuators move the tops of Wall W1 and Wall W2 to the new calculated X_1 and X_2 displacements. Note that it is important that the new positions are obtained simultaneously and this is achieved by subdividing the time step into 10 equal time increments and sending the actuators to $X_{old} + n \cdot (X_{new} - X_{old}) / 10$ at each increment where n increases from 1 to 10 at corresponding increments. At the end of the time increment the forces F_1 and F_2 are measured. Thus, all the information assumed known at time T is now known at time T+ΔT and so the process can continue.

7.3 2DOF System – separated

A sketch comparing the test setup for a separated and non-separated PD test is shown in Figure 6. In a separated PD test the walls are not built on top of one another but as separate single-storey walls. The above equations can be used for this modified structure if two changes are made to the program as discussed further on. Thus, the horizontal load transfer between the two walls is simulated.



(a) Separated - the sum of the two separate walls



(b) Not Separated

Figure 6: Sketch Illustrating the Difference Between a Separated and Non-Separated Two-storey PD Test

1. In a two-level structure, the shear force over the first storey = $F_1 + F_2$. Thus, if the deflection of the lower wall of the two-storey structure is to equal the deflection of the same wall if the walls are tested separated, then the force actually being applied to the single lower wall in the separated structure must also = $F_1 + F_2$. Hence, to obtain the correct value of the force (F_1) in Eqn.(10) the program uses the actual measured force applied to the separated lower wall ($F_1 + F_2$) minus the actual measured force applied to the separated upper wall (F_2) giving $(F_1 + F_2) - F_2 = F_1$ as required; i.e. F_1 in Eqn.(10) is replaced with $F_1 - F_2$.
2. The solutions to the equations in Section 7.3 are X_1 and X_2 . For a two-storey structure the actuators move the walls to these deflections. However, for a separated structure, the actuator at mass M_2 has to be sent to $(X_2 - X_1)$, to impose the required inter-storey displacement.

7.4 Torsional Response of a Simplified Non-symmetric House

The structure is a single-storey simulated house as sketched in Figure 1(c). In the PD test actuators are to be used along the lines of Wall W1 and Wall W2 as shown. The analyses subsequently performed in this report used overall house dimension of $D=B=12\text{m}$ and stiffnesses and masses appropriate to a New Zealand house and that satisfy NZS 3604:1999

[5]. The house is assumed to have a rigid ceiling diaphragm and the earthquake is assumed to be parallel to Wall W1 and Wall W2 – i.e. parallel to the X axis. Wall W1 is taken to be stronger and stiffer than Wall W2 and hence diaphragm rotation is expected. This will be resisted by the perpendicular walls (Wall W3 and Wall W4). In the analysis presented it is assumed that Wall 3 and Wall 4 remain elastic with stiffness K. They will impose a torsional restraint of magnitude $K_R \times \Phi$ to partially resist the diaphragm rotation where Φ is the diaphragm rotation. It can be shown that $K_R = 0.5K \cdot D^2$.

The analysis below considers an increment of earthquake acceleration applied over a small time step. During this time step all walls are considered to be perfectly elastic. At the end of the time increment wall stiffnesses are reassessed. Thus the methodology can be applied to non-linear systems.

Consider a vertical Z axis passing through the centre of mass, M shown in Figure 1. The moment of inertia of the floor about the axis is taken to be I_0 . If the total mass M is distributed uniformly over the plan then $I_0 = M(B^2+D^2)/12$ [16].

The movement of Mass M_1 in the X direction and its rotation about the Z axis is taken as (X,θ) . (As there is no excitation in the Y direction and the walls in this direction are symmetric about the centre of mass, the Y movement is zero and can be excluded from the equations of motion.)

For a ground excitation of \ddot{G}_x , Chopra [16] showed that the equations of motion could be expressed as:

$$\begin{bmatrix} M & 0 \\ 0 & I_0 \end{bmatrix} \begin{Bmatrix} \ddot{X} \\ \ddot{\mathbf{q}} \end{Bmatrix} + \begin{bmatrix} C_{11} & C_{12} \\ C_{21} & C_{22} \end{bmatrix} \begin{Bmatrix} \dot{X} \\ \dot{\mathbf{q}} \end{Bmatrix} + \begin{bmatrix} K_1 + K_2 & K_1 D_1 - K_2 D_2 \\ K_1 D_1 - K_2 D_2 & K_1 D_1^2 + K_2 D_2^2 + K_R \end{bmatrix} \begin{Bmatrix} X \\ \mathbf{q} \end{Bmatrix} = -M \begin{Bmatrix} \ddot{G}_x \\ 0 \end{Bmatrix}$$

Thus, $C_{11} = \alpha \cdot M + \beta \cdot (K_1 + K_2)$
 $C_{12} = \beta \cdot (K_1 D_1 - K_2 D_2)$
 $C_{21} = \beta \cdot (K_1 D_1 - K_2 D_2)$
 $C_{22} = \alpha \cdot I_0 + \beta \cdot (K_1 D_1^2 + K_2 D_2^2 + K_R)$

The equations of motion from the above matrix equation are:

$$\ddot{X} = -\ddot{G}_x - (C_{11} \dot{X} + C_{12} \dot{\mathbf{q}} + (K_1 + K_2)X + (K_1 D_1 - K_2 D_2)\mathbf{q}) / M$$

$$ie., \ddot{X} = -\ddot{G}_x - (C_{11} \dot{X} + C_{12} \dot{\mathbf{q}} + K_1(X + D_1\mathbf{q}) + K_2(X - D_2\mathbf{q})) / M$$

$$or, \ddot{X} = -\ddot{G}_x - (C_{11} \dot{X} + C_{12} \dot{\mathbf{q}} + F_1 + F_2) / M \dots\dots\dots(12)$$

$$Also I_0 \ddot{\mathbf{q}} = -(C_{21} \dot{X} + C_{22} \dot{\mathbf{q}} + X(K_1 D_1 - K_2 D_2) + \mathbf{q}(K_1 D_1^2 + K_2 D_2^2 + K_R))$$

$$ie., I_0 \ddot{\mathbf{q}} = -(C_{21} \dot{X} + C_{22} \dot{\mathbf{q}} + D_1 \cdot K_1 (X + D_1 \mathbf{q}) - D_2 \cdot K_2 (X - D_2 \mathbf{q}) + \mathbf{q} \cdot K_R)$$

$$or, I_0 \ddot{\mathbf{q}} = -(C_{21} \dot{X} + C_{22} \dot{\mathbf{q}} + D_1 \cdot F_1 - D_2 \cdot F_2 + \mathbf{q} \cdot K_R) \dots\dots\dots(13)$$

It can be seen from eqns (12) and (13) that the calculations are not directly a function of the wall stiffness but are instead a function of the forces F_1 and F_2 in the walls, which are also the forces in the actuator load cells.

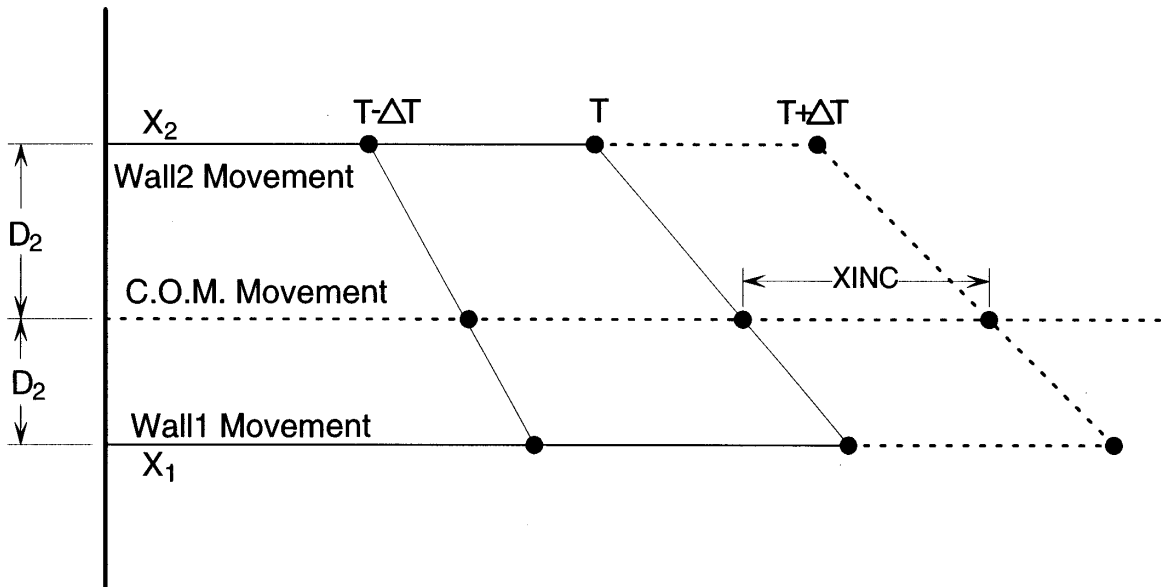


Figure 7: Analysis Theory - House Torsional Response

If the analysis has proceeded up to time T as sketched in Figure 7, and the rotational and linear velocities and displacements at the centre of mass are known at this time then the rotational and linear accelerations at the start of the time step can be computed from the equations in Figure 5. If the movement at the centre of mass is known then the deflections of the walls (i.e., X_1 for Wall W1 and X_2 for Wall W2) can be obtained from:

$$X_1 = X + D_1 \mathbf{q} \quad \text{and} \quad X_2 = X - D_2 \mathbf{q} \quad \dots \dots \dots (14)$$

The computer controlling the PD process then sends a signal to make Actuator 1 move Wall W1 to X_1 and Actuator 2 move Wall W2 to X_2 . When the movement is completed, and at the end of the time step, the forces F_1 and F_2 in the two actuators are measured. Thus, all the information assumed known at time T is now known at time $T+\Delta T$ and so the process can continue.

Note that the natural periods of translational (T_1) and rotational modes (T_2) are obtained from:

$$T_1 = 2\pi \sqrt{M / (K_1 + K_2)} \quad \text{and} \quad T_2 = 2\pi \sqrt{I_0 / (K_2 D_2^2 + K_2 D_2^2 + K_R)} \quad \dots \dots \dots (15)$$

The moment of inertia of the floor about the axis (I_0) in the Excel and PD models was taken as $I_0 = M(B^2 + D^2)/12$ [16]. This effectively assumed that the total mass M was distributed uniformly over the floor plan as shown by the calculation below.

$$\begin{aligned} I_0 &= \mathbf{r} \int r^2 dA = \mathbf{r} \int (x^2 + y^2) dA = \mathbf{r} \int x^2 dA + \mathbf{r} \int y^2 dA = \mathbf{r} [Bx^3 / 3]_{-D/2}^{D/2} + \mathbf{r} [Dx^3 / 3]_{-B/2}^{B/2} = \\ &= \mathbf{r} [BD^3 + DB^3] / 12 = M [D^2 + B^2] / 12 \end{aligned}$$

The Ruaumoko model [3] requires masses to be specified at nodes. A moment of inertia of I_0 can be achieved if $1/6^{\text{th}}$ of the total mass is placed at the centreline of each side in the Ruaumoko model and the remaining $1/3^{\text{rd}}$ of the total mass is placed at the house centreline, as shown below:

$$I_0 = M \left[2 \left\{ \frac{D}{2} \right\}^2 + 2 \left\{ \frac{B}{2} \right\}^2 \right] / 6 = M [D^2 + B^2] / 12$$

7.5 2DOF Torsion System With Perpendicular Walls of Same Properties

The structure in Figure 1(c) is taken to have Wall W3 identical to Wall W1 and Wall W2 identical to Wall W4. Two earthquake directions, where the earthquake strikes at 45° to the house main axes, are shown in this figure. For an earthquake in direction EQ1 the wall resistance is symmetrical to this angle of attack and there will be no diaphragm rotation. However, for an earthquake in direction EQ2 the diaphragm will rotate. This situation is considered in the analysis following where an X and Y direction modified El Centro earthquake act concurrently but with earthquake magnitude reduced by $\sqrt{2}$ in each direction. The general equation of motion is:

$$\begin{bmatrix} M & 0 & 0 \\ 0 & M & 0 \\ 0 & 0 & I_0 \end{bmatrix} \begin{Bmatrix} \ddot{X} \\ \ddot{Y} \\ \ddot{\mathbf{q}} \end{Bmatrix} + \begin{bmatrix} C_{11} & C_{12} & C_{13} \\ C_{21} & C_{22} & C_{23} \\ C_{31} & C_{32} & C_{33} \end{bmatrix} \begin{Bmatrix} \dot{X} \\ \dot{Y} \\ \mathbf{q} \end{Bmatrix} + \begin{bmatrix} K_1 + K_2 & 0 & K_1 D_1 - K_2 D_2 \\ 0 & K_1 + K_2 & K_1 D_1 - K_2 D_2 \\ K_1 D_1 - K_2 D_2 & K_1 D_1 - K_2 D_2 & 2(K_1 D_1^2 + K_2 D_2^2) \end{bmatrix} \begin{Bmatrix} X \\ Y \\ \mathbf{q} \end{Bmatrix} = -M \begin{Bmatrix} \ddot{G}_x \\ \ddot{G}_y \\ 0 \end{Bmatrix} \dots\dots\dots(16)$$

Thus: $C_{11} = \alpha.M + \beta.(K_1 + K_2) = C_{22}$
 $C_{12} = 0 = C_{21}$
 $C_{13} = \beta.(K_1 D_1 - K_2 D_2) = C_{23} = C_{31} = C_{32}$
 $C_{33} = \alpha.I_0 + 2\beta.(K_1 D_1^2 + K_2 D_2^2)$

But: $\ddot{G} = \ddot{G}_x = \ddot{G}_y$. By symmetry $\dot{X} = \dot{Y}$ and $X = Y$.

Hence, the first matrix equation expands to:

$$\ddot{X} = -\ddot{G} - (C_{11} \dot{X} + C_{13} \dot{\mathbf{q}} + (K_1 + K_2)X + (K_1 D_1 - K_2 D_2)\mathbf{q}) / M$$

$$\text{ie., } \ddot{X} = -\ddot{G} - (C_{11} \dot{X} + C_{13} \dot{\mathbf{q}} + K_1(X + D_1 \mathbf{q}) + K_2(X - D_2 \mathbf{q})) / M$$

$$\text{or, } \ddot{X} = -\ddot{G} - (C_{11} \dot{X} + C_{13} \dot{\mathbf{q}} + F_1 + F_2) / M \dots\dots\dots(17)$$

The second matrix equation is:

$$\ddot{Y} = -\ddot{G} - (C_{11} \dot{Y} + C_{13} \dot{\mathbf{q}} + F_1 + F_2) / M \dots\dots\dots(18)$$

The third matrix equation is:

$$I_0 \ddot{\mathbf{q}} = -(C_{31} \dot{X} + C_{32} \dot{Y} + C_{33} \dot{\mathbf{q}} + X(K_1 D_1 - K_2 D_2) + Y(K_1 D_1 - K_2 D_2)) + 2\mathbf{q}(K_1 D_1^2 + K_2 D_2^2)$$

$$\text{ie., } I_0 \ddot{\mathbf{q}} = -(2C_{31} \dot{X} + C_{33} \dot{\mathbf{q}} + 2D_1 \cdot K_1 (X + D_1 \cdot \mathbf{q}) - 2D_2 \cdot K_2 (X - D_2 \cdot \mathbf{q}))$$

$$\text{or, } I_0 \ddot{\mathbf{q}} = -(2C_{13} \dot{X} + C_{33} \dot{\mathbf{q}} + 2D_1 \cdot F_1 - 2D_2 \cdot F_2) \dots\dots\dots (19)$$

8. VERIFICATION OF PROGRAM BY SDOF TESTS

The structure being considered is illustrated in Figure 1(a). To investigate whether PD tests can be simulated using ITHA with the Ruaumoko software, the walls described in Table 1 were:

- (1) cyclically racked under an increasing deflection regime.
- (2) tested under a PD regime to the modified El Centro earthquake.
- (3) analysed by ITHA to the modified El Centro earthquake using the results of Step (1) above to model the walls using the Stewart [11] hysteresis loop model.

Table 1: Single Walls Tested

Name	Description of Wall Tested
Wall W1	1.2 m standard plasterboard wall with 3 nails in P21 uplift restraint.
Wall W2	2.4 m standard plasterboard wall with 3 nails in P21 uplift restraint.
Wall W3	2.4 m plywood wall with 3 nails in P21 uplift restraint.
Wall W4	2.4 m plywood wall with 6 nails in P21 uplift restraint.

The timber framing for the walls was constructed to NZS 3604:1999. The timber for the top and bottom plates was nominal 100 x 50 mm radiata pine and the timber for the studs was nominal 90 x 35 mm Radiata Pine. Studs were at 600 mm centres. Each end of each stud was nailed to the plates with three 90 x 3.15 mm power-driven nails. The bottom plate was nailed to the “foundation beam” with groups of three 90 x 3.15 mm power-driven nails at 600 mm centres.

A P21 uplift restraint [18] was used at each end of the test walls. This consisted of a 400 mm long block of 100 x 50 mm radiata pine restrained from uplift and nailed to the end studs of the wall with either three or six 100 x 4 mm bright flathead nails.

Plasterboard Walls

The 9.5 mm standard paper-faced gypsum plasterboard was nailed to the studs using 30 x 2.8 mm proprietary nails. These were at 150 mm centres around the edges of the sheets, with pairs at 300 mm centres down the centre stud. End nails were at 50 mm from the edge of the sheet at all sheet corners.

Plywood walls

The 7 mm grade D-D plywood sheets were attached to the framing using 30 x 2.5 mm galvanised clouts at 150 mm centres around the outside of the sheets, and 300 mm centres down the centre of the sheets.

8.1 Results

The test cyclic hysteresis loops and matched Stewart [11] hysteresis analytical model loops for corresponding walls are shown in Figure 8-11. The Stewart hysteresis model gives a reasonable approximation of test data. For walls which tested to be stronger in one direction than the other the analysed model approximately matches the average properties of a symmetrical wall. There is a reasonable agreement between the two curves in each plot.

Applied force versus deflection relationships were plotted from test measurements. A comparison with ITHA hysteresis model loops is given in Figure 13-16 for Wall W1 to Wall W4 respectively for excitation from 1.0 level of the El Centro excitation discussed above. Note that the walls had already been subjected to 0.5 level of the El Centro excitation in both the PD and ITHA. Generally moderate agreement was obtained.

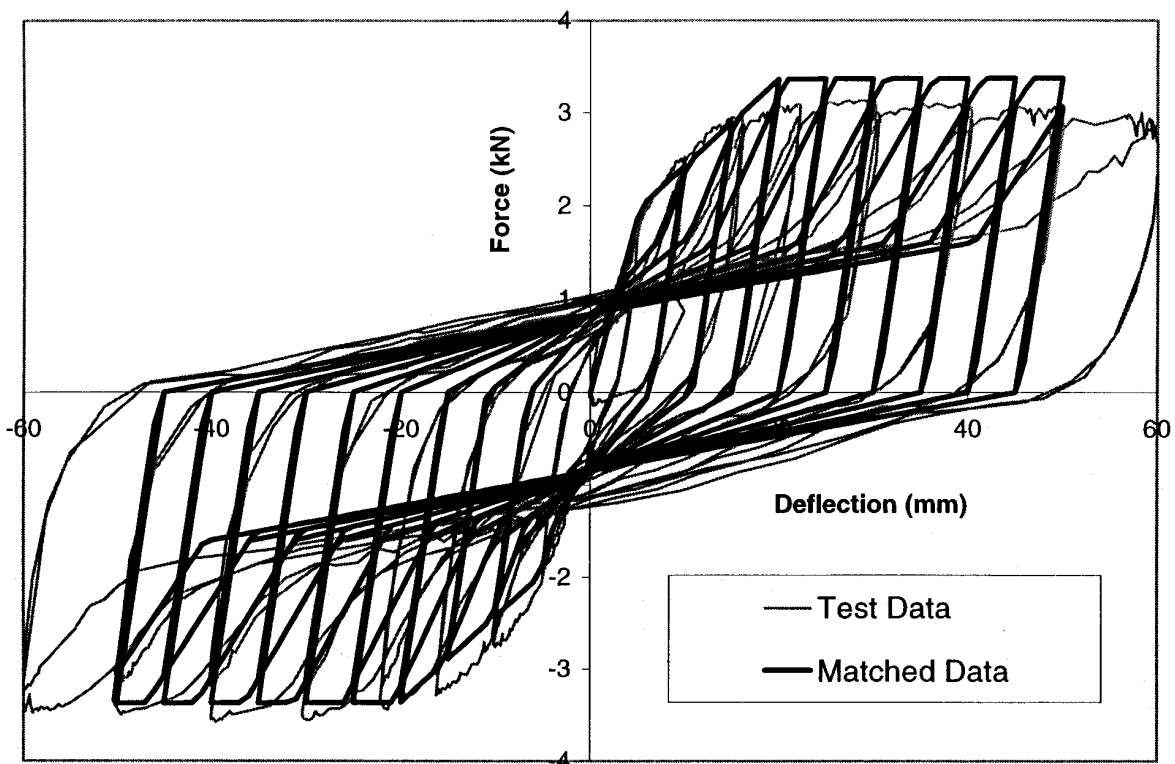


Figure 8: Wall W1. Cyclic Test and Ruamoko Modelled Hysteresis Loops

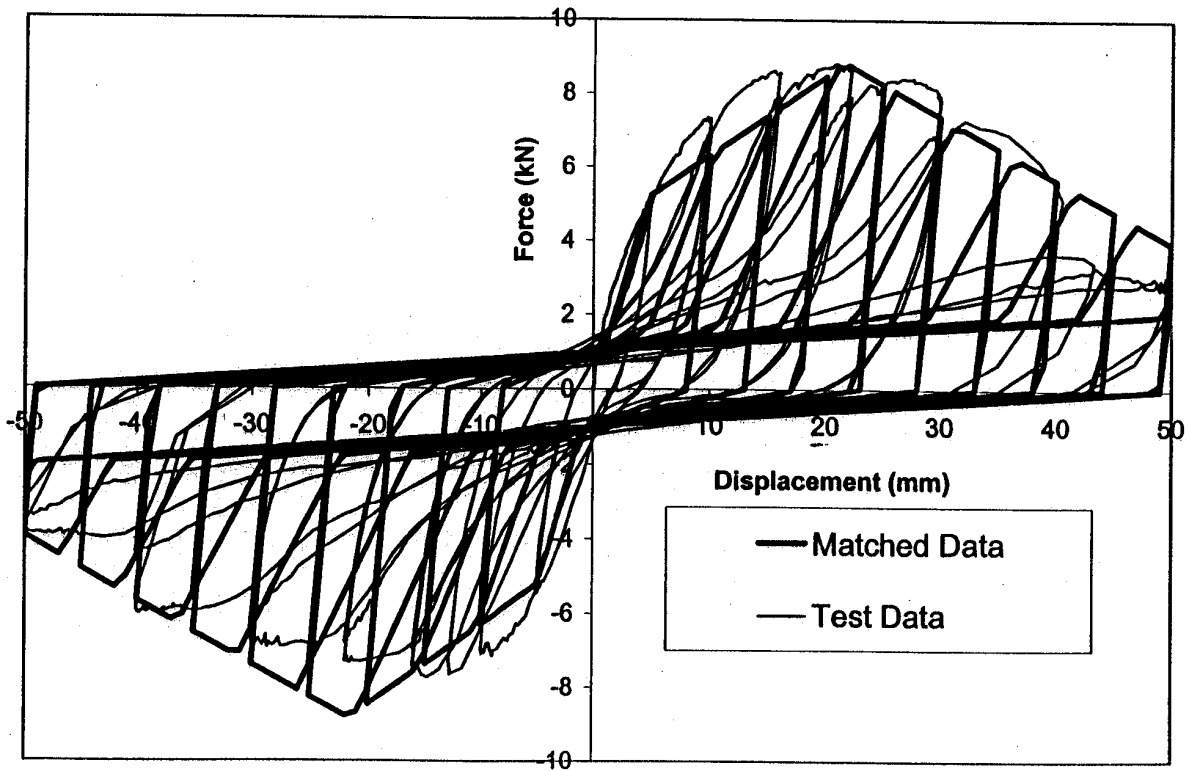


Figure 9: Wall W2. Cyclic Test and Ruaumoko Modelled Hysteresis Loops

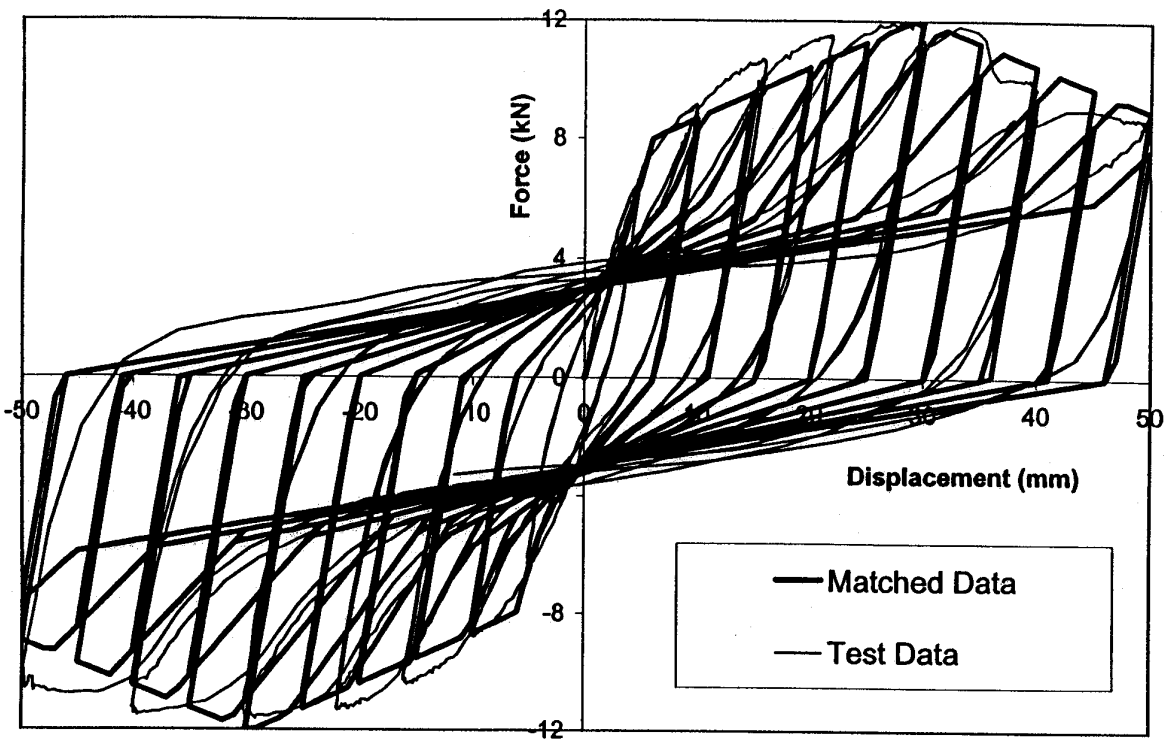


Figure 10: Wall W3. Cyclic Test and Ruaumoko Modelled Hysteresis Loops

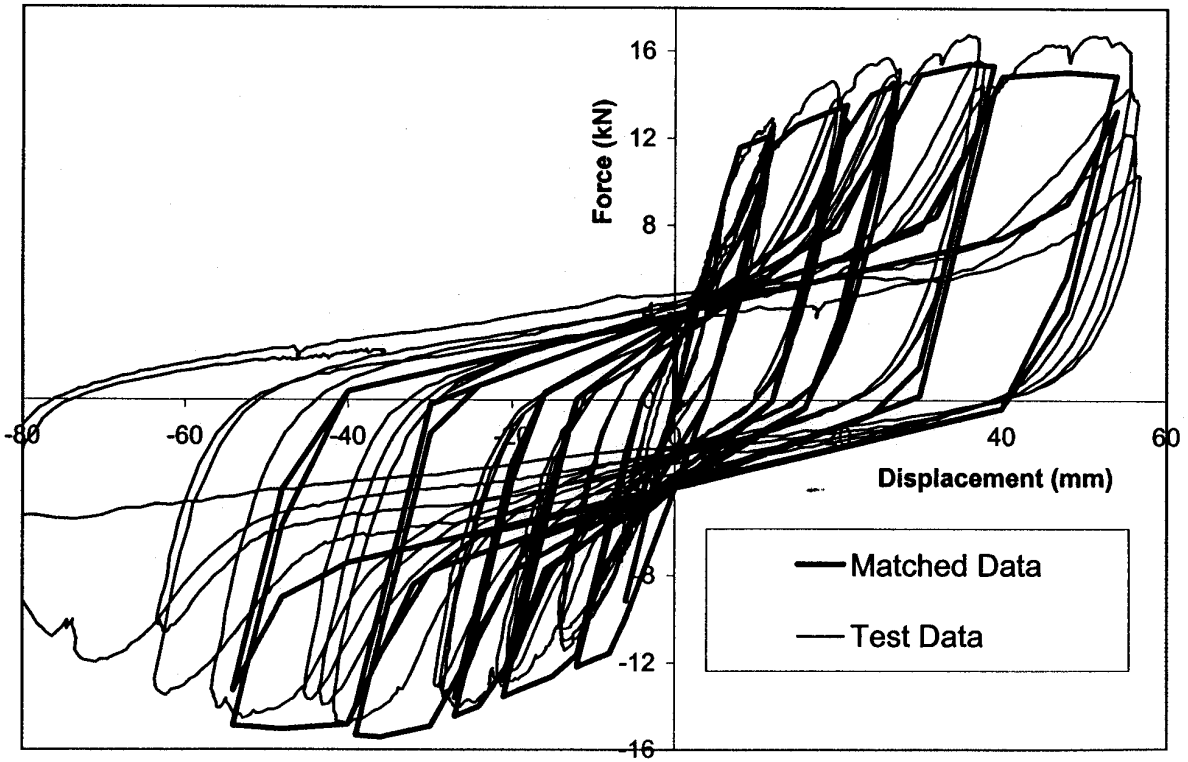


Figure 11: Wall W4. Cyclic Test and Ruaumoko Modelled Hysteresis Loops

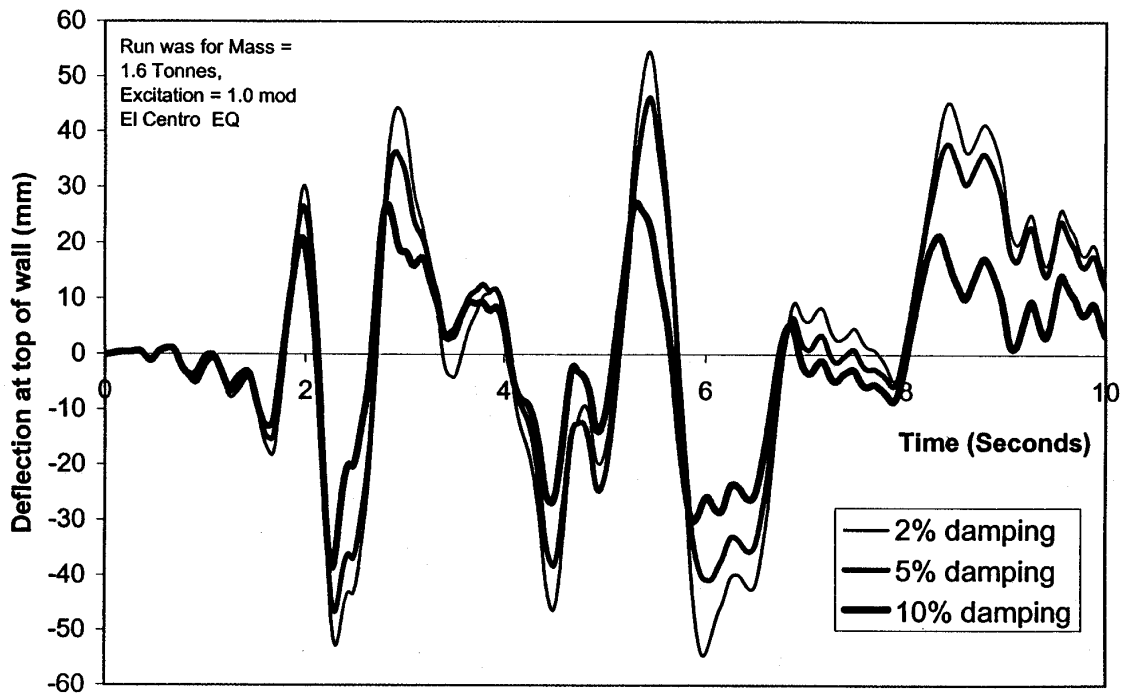


Figure 12: Deflections Computed Using Different Levels of Damping

The ultimate deflection experienced by a wall in an earthquake is the best indicator of the distress experienced by the wall. The remainder of this report compares the time history of deflections measured in a PD test and predicted by ITHA. This time sequence also allows easier visual comparison of the two methods in the plots than the hysteresis loops comparison of Figures 13-16.

All the PD tests on single walls used an input initial stiffness $K = 1000$ N/mm. The program only uses K to compute the damping constant, C , of Equation (1). A damping ratio of 5% critical was used in the PD runs. However, in the Ruaumoko runs the initial stiffnesses to match the cyclic test loops were $K_R = 374, 1076, 1327$ and 1523 N/mm for the four single walls tested as listed above. Thus, to obtain the same damping value C as used in the PD runs, the ITHA damping was changed to $5 \cdot \sqrt{1000/K_R} = 8.18, 4.83, 4.35$ and 4.05 percent for the 4 walls of Table 1. The amount of damping influences the interstorey deflections as illustrated in Figure 12.

The PD tests were performed at a ratio of 16 real time to simulated time. Where noted, only simulated times are given.

A comparison of the deflections measured in the PD test and that determined from the Ruaumoko simulation are given in the Figures listed in Table 2. This table also shows the testing program imposed on each wall. The ITHA runs simulated the whole time history of loading but the comparison is only presented for the final loading. Thus, the ITHA run for the comparison in Figure 23 for Wall W3 under 1.0 El Centro earthquake imposed a train of 0.25, 0.5 and 1.0 El Centro earthquakes, with each “carriage” separated by five seconds of zero accelerations. However, Figure 23 only shows the deflections for the 1.0 El Centro earthquake portion.

8.2 Description of Damage

After the 1.0 El Centro earthquake had been imposed on Wall W1 the nails heads were embedded into the plasterboard sheet along the base and partially up the ram end of the wall. This became more extreme after imposition of 1.25 El Centro earthquake and the specimen deflection became very non-symmetric with one end of the wall having degraded faster than the other.

Greater damage occurred during excitation of Wall W2 with 1.0 El Centro earthquake than for the 1.2 m long Wall W1 under the same excitation. The wall effectively failed under the first major pulse under 1.25 El Centro earthquake and the imposed deflection exceeded ram capacity.

The main deformation mechanism of Wall W3 was uplift from the foundation beam and observed slip between plywood and frame (using pencil lines) was small. Under excitation from 1.0 El Centro earthquake the bottom plate split at approximately six seconds when the excellent agreement with the Ruaumoko simulation subsequently decreased. However, as the plywood appeared to experience little damage the wall was upended and a new P21 restraint with six nails constructed. This wall was subsequently called Wall W4.

The damage observed with Wall W4 was both nail head rotation and uplift of the bottom plate under 1.0 El Centro earthquake. This increased with seven nails partially withdrawing under 1.25 El Centro earthquake.

8.3 Conclusions

Using the Stewart [11] model a good match was obtained between slow cyclic hysteresis loops and the Ruaumoko input model.

Generally a very good agreement was obtained between the ITHA simulations and the PD test deflections – particularly for plywood. This agreement was poorer for plasterboard - particularly the 1.2 m long specimen for which the slow cyclic hysteresis loops were unusual in that no decay was measured, even at the larger deflections.

The agreement between ITHA simulation and PD test was best when the excitation level resulted in maximum deflections between 20-40 mm. At lower excitation levels the ITHA remained effectively elastic whereas the PD specimens became inelastic and gave a more sluggish response. It is likely that this difference is due to a less precise match between the cyclic measured response and the Stewart [11] model for small (0-20 mm) response.

At large imposed deflections the PD test specimens tended to drift to one side – particularly for plasterboard specimens. This is attributed to the Stewart [11] Ruaumoko model match being symmetric, whereas the test specimen rarely is, as evidenced by the slow cyclic hysteresis loops. Further, at large deflections the test specimen behaviour tends to vary significantly between specimens.

If the Stewart [11] Ruaumoko model match for large and small deflections varies from the actual test specimen, then the PD test is considered to be more realistic than Ruaumoko modelling and would best represent actual field behaviour.

Table 2: Comparison of Deflections Measured in PD Testing and Ruaumoko Simulation of SDOF Walls

Wall Type	Figure No. for Cyclic Testing	Figure No. for PD and ITHA Hysteresis Comparison	Figure No. for PD and ITHA Deflection Comparison	Mass (Tonnes) Imposed	Factor used on El Centro Earthquake
1	Figure 8	Figure 13		1.6	0.25
1			Figure 17	1.6	0.5
1			Figure 18	1.6	1.0
1			Figure 19	1.6	1.25
2	Figure 9	Figure 14		3.0	0.25
2			Figure 20	3.0	0.5
2			Figure 21	3.0	1.0
2				3.0	1.25
3	Figure 10			4.5	0.25
3			Figure 22	4.5	0.5
3		Figure 15	Figure 23	4.5	1.0
4	Figure 11		Figure 24	4.5	1.0
4		Figure 16	Figure 25	4.5	1.5

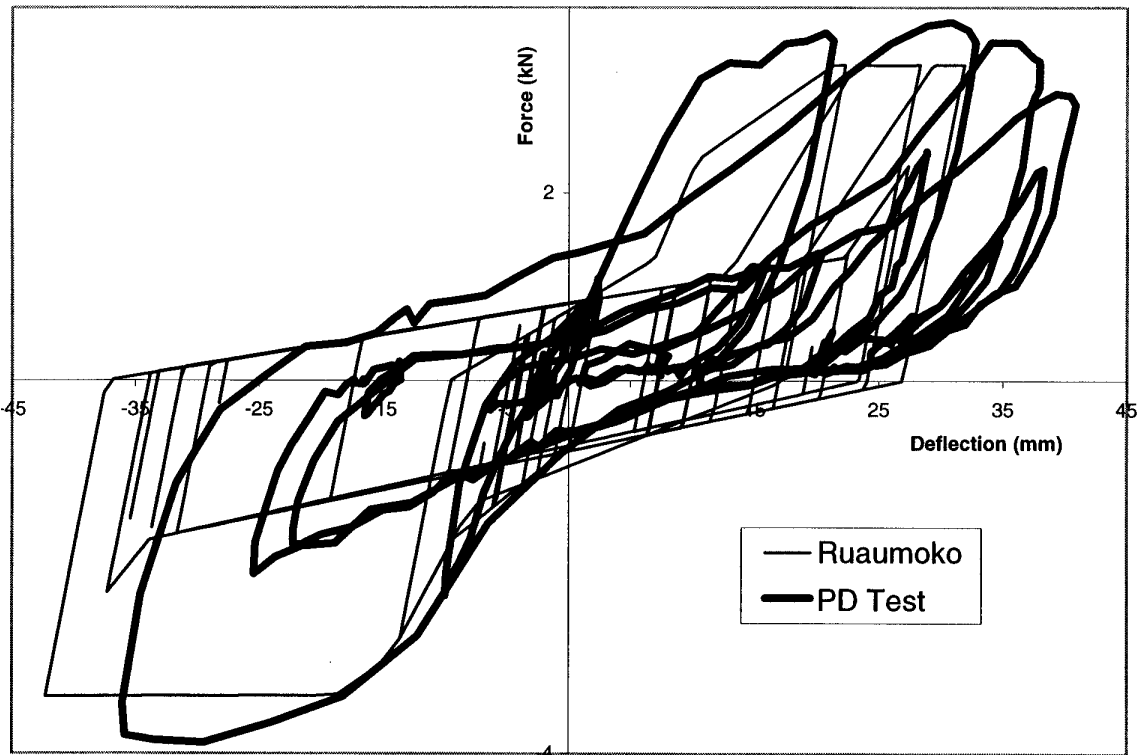


Figure 13: Wall W1. PD Test and ITHA Hysteresis Loops

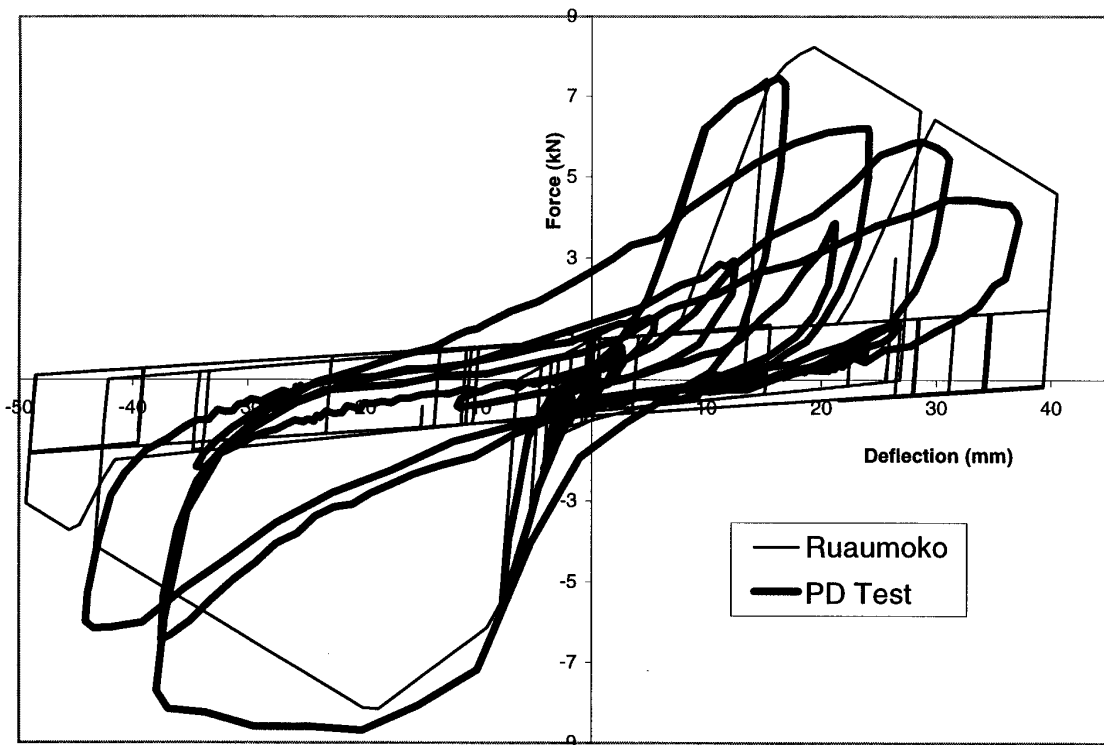


Figure 14: Wall W2. PD Test and ITHA Hysteresis Loops

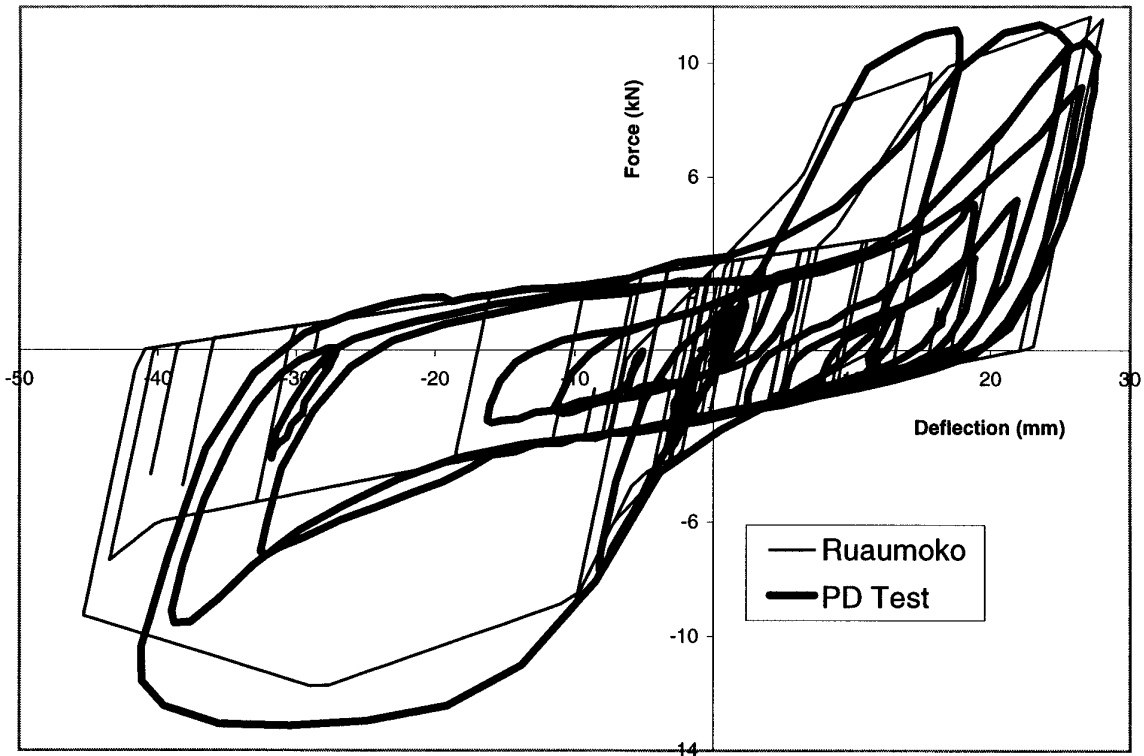


Figure 15: Wall W3. PD Test and ITHA Hysteresis Loops

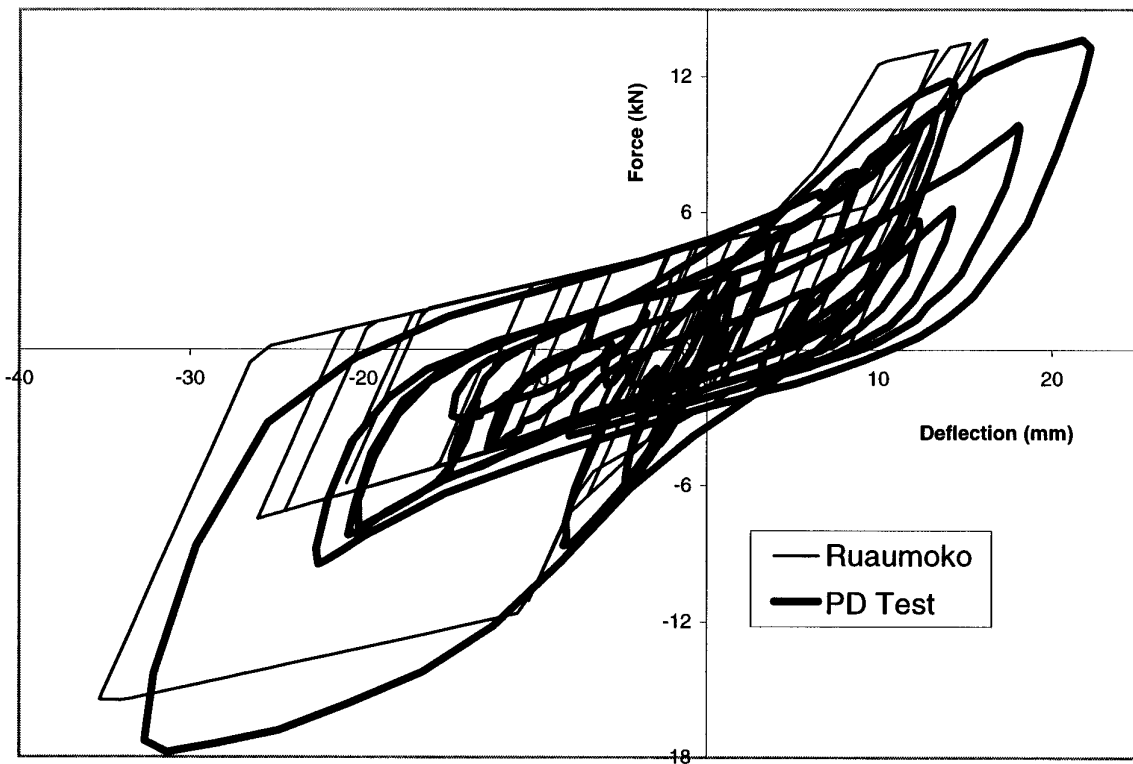


Figure 16: Wall W4. PD Test and ITHA Hysteresis Loops

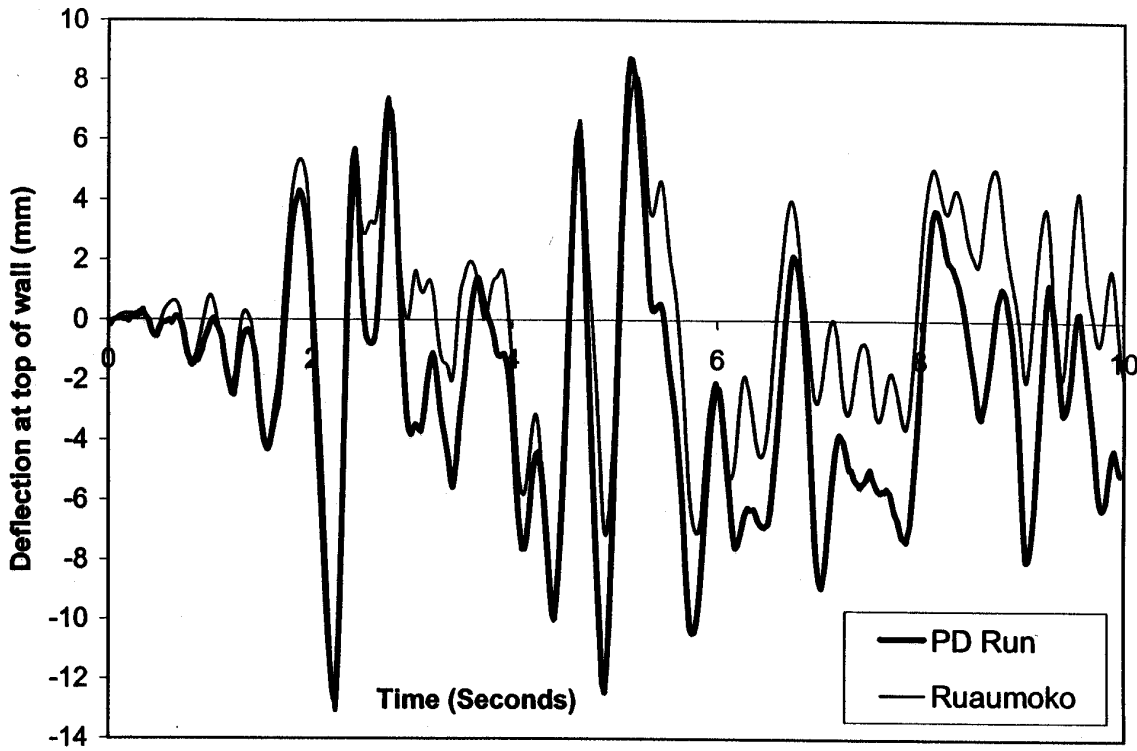


Figure 17: Comparison Ruaumoko and PD. Wall W1, 0.5 El Centro EQ

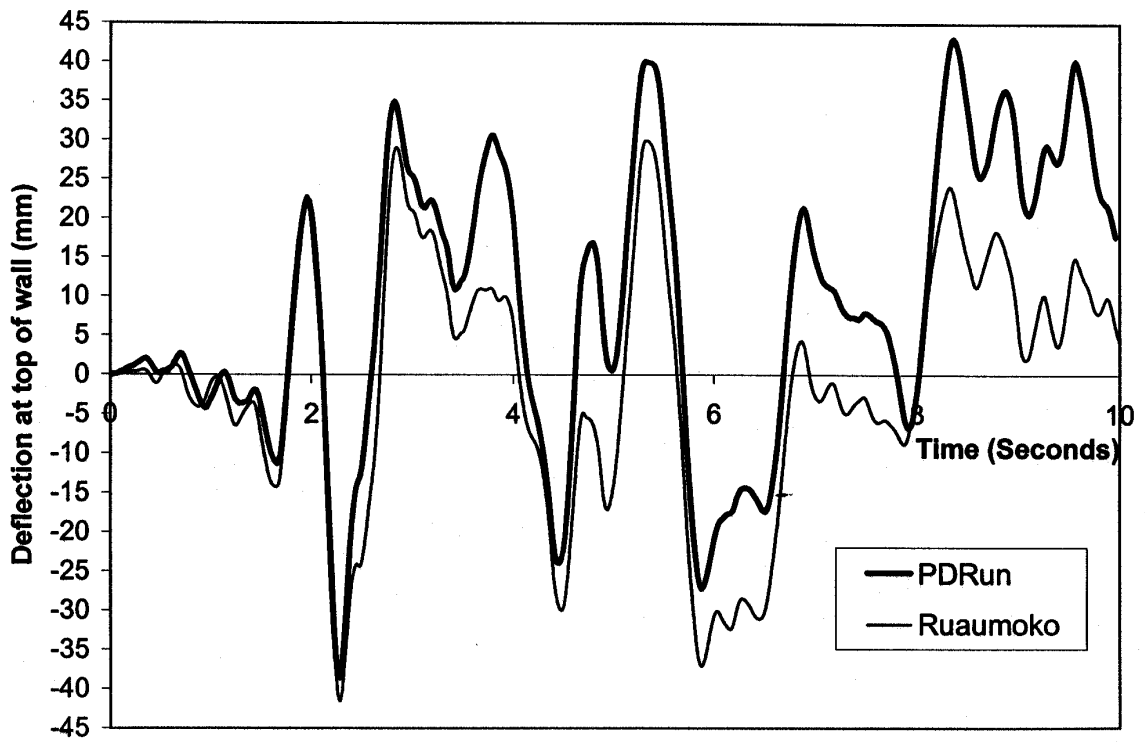


Figure 18: Comparison Ruaumoko and PD. Wall W1, 1.0 El Centro EQ

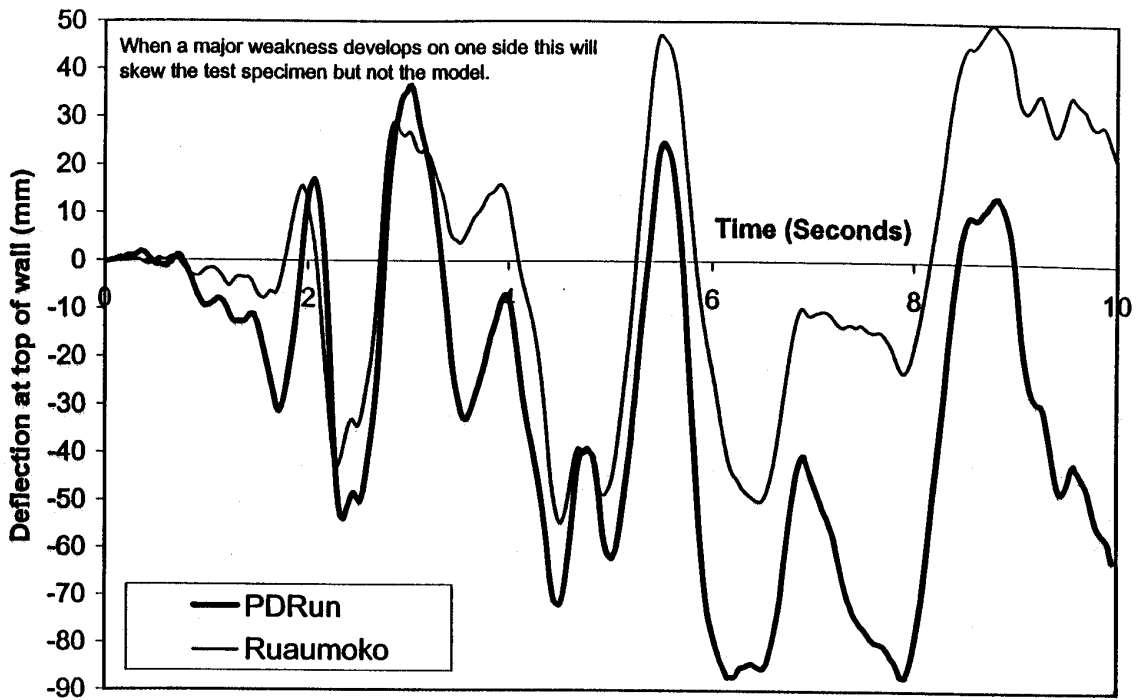


Figure 19: Comparison Ruaumoko and PD. Wall W1, 1.25 El Centro EQ

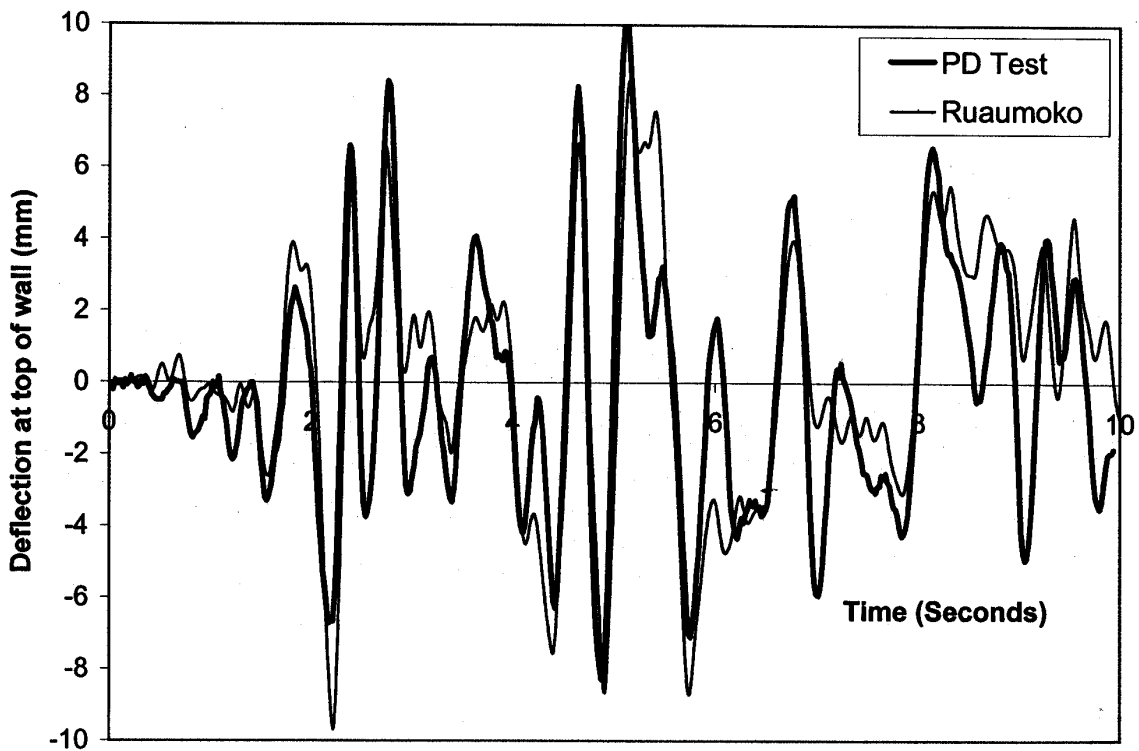


Figure 20: Comparison Ruaumoko and PD. Wall W2, 0.5 El Centro EQ

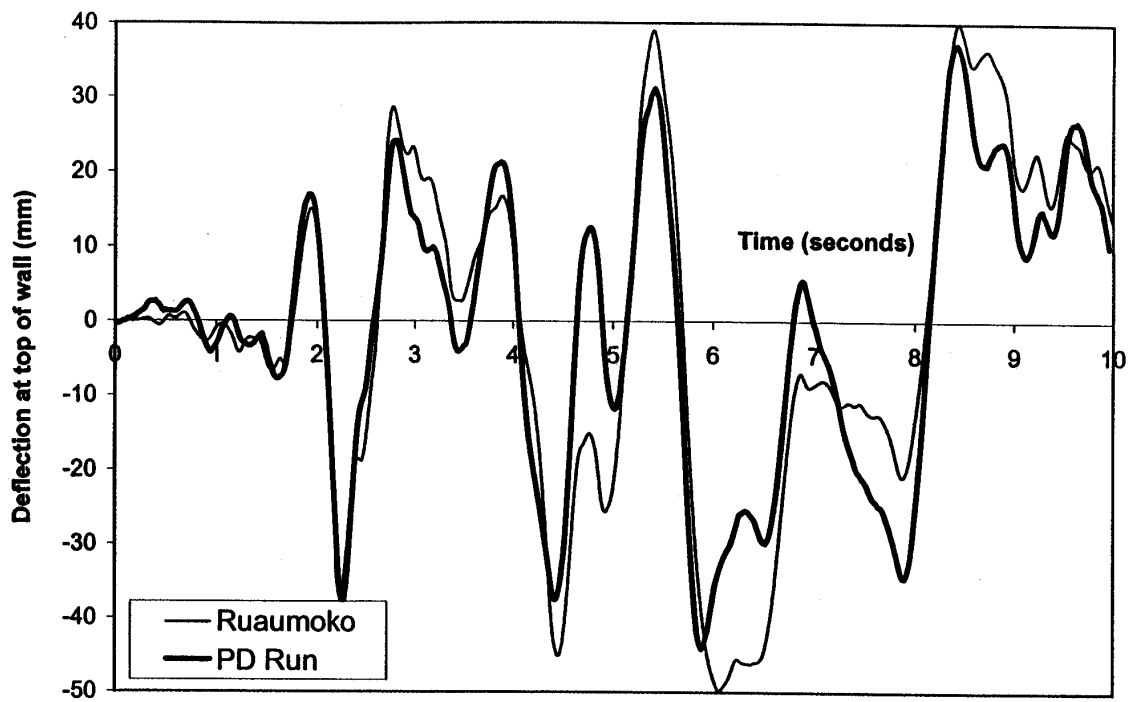


Figure 21: Comparison Ruaumoko and PD. Wall W2, 1.0 El Centro EQ

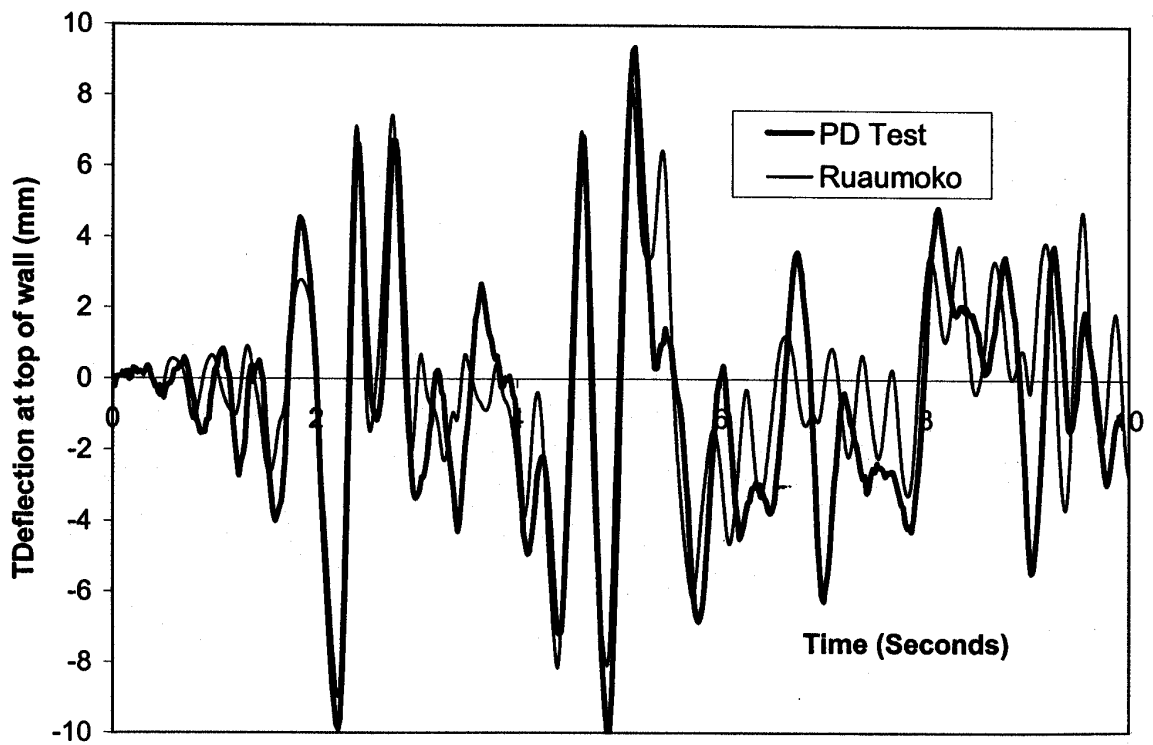


Figure 22: Comparison Ruaumoko and PD. Wall W3, 0.5 El Centro EQ

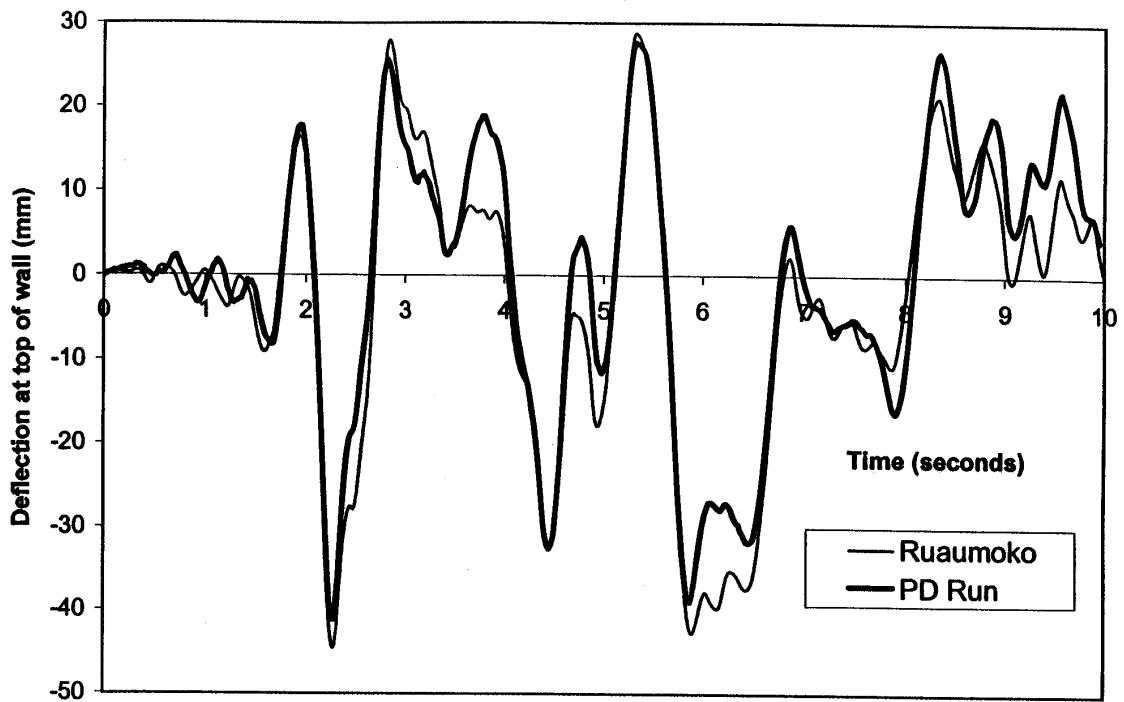


Figure 23: Comparison Ruaumoko and PD. Wall W3, 1.0 El Centro EQ

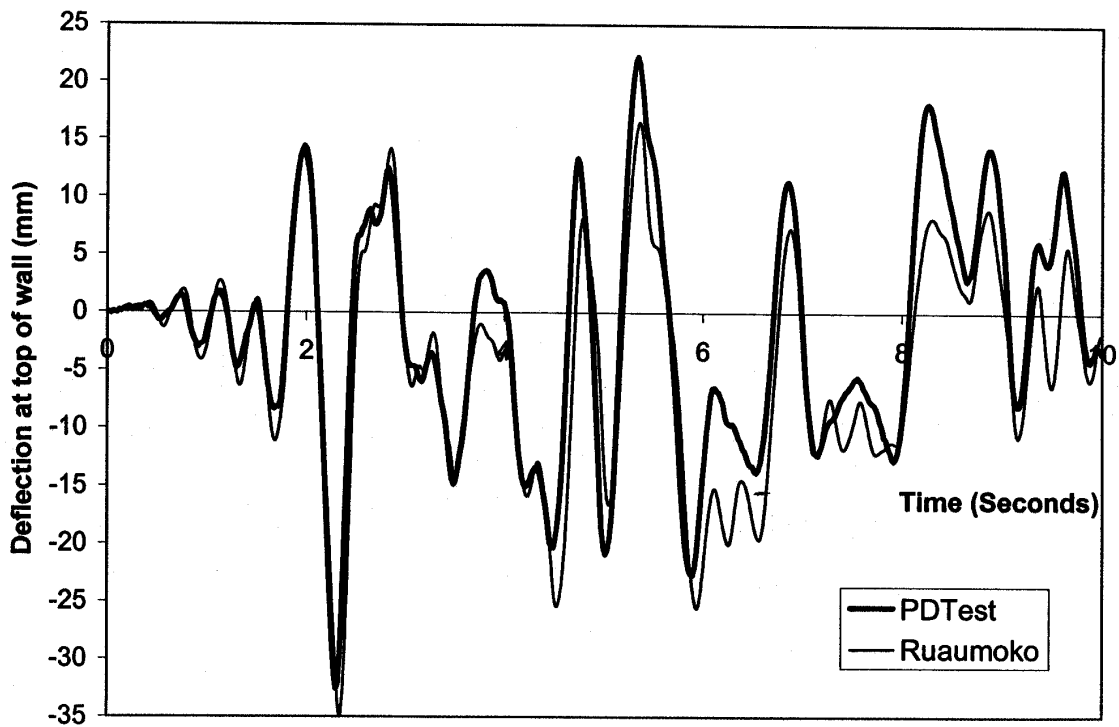


Figure 24: Comparison Ruaumoko and PD. Wall W4, 1.0 El Centro EQ

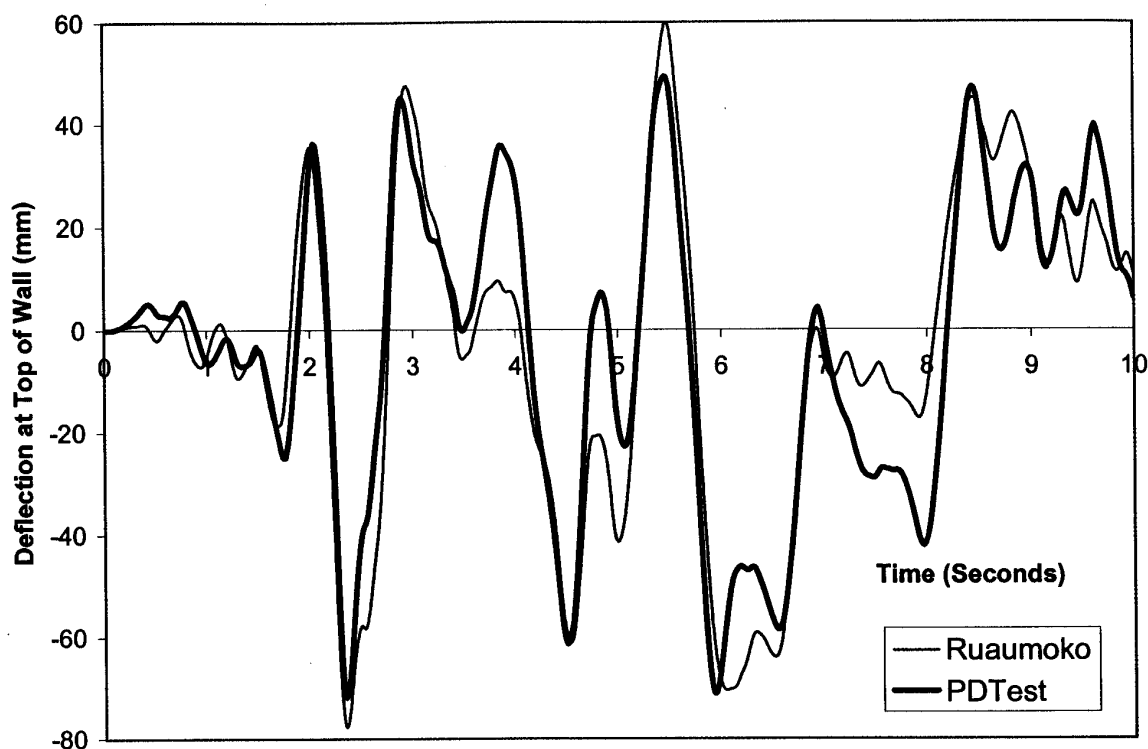


Figure 25: Comparison Ruaumoko and PD. Wall W4, 1.5 El Centro EQ

9. VERIFICATION OF PROGRAM BY TWO DEGREES OF FREEDOM TESTS

9.1 Construction

The tests in this series used three types of single-storey walls PD-tested in pairs as a 2DOF separated test as described in Section 7.3. The three types of single walls are summarised in Table 3.

Table 3: Two-storey Walls PD-Tested as Separated Walls

Name	Description of Wall Tested
Wall5	1.2 m x 1.2 m wall plywood wall with three nails in P21 uplift restraint.
Wall6	As per Wall W4 of Table 1 but with variations described below.
Wall7	As per Wall6 but on same wall and subsequent to tests on WallSetD.

It had been intended that Wall W4 and Wall W6 be the same. The construction and testing described in Section 8 was done at an earlier date, by a different technician and used a different batch of timber. It was subsequently found that the bottom plate was nailed to the foundation beam with two 100 x 4 mm nails at 600 mm centres rather than the groups of three 90 x 3.15 mm power-driven nails at 600 mm centres used with Wall W4. This is likely to have affected the hold-down performance. Wall W6 deformation tended to be dominated more by uplift than Wall W4 and showed a small separation between the top plate and studs which did not occur with Wall W4. A comparison between PD test and Ruaumoko simulation for the series of tests in this section did not show close agreement when the simulation used the hysteresis loops of Wall W4. Consequently, a further specimen was made using the same construction as Wall W6

and cyclically tested. A comparison between the test cyclic hysteresis loops and matched Stewart [11] hysteresis Ruaumoko model loops for Wall W6 is shown in Figure 26. The subsequent comparison between Ruaumoko using Wall W6 loops and PD was good, as discussed below.

Wall W5 is the same construction as Wall W6 except that the wall was only 1.2 m high and 1.2 m wide and was covered by a single half-height sheet. The P21 end restraint used three nails. A comparison between the test cyclic hysteresis loops and matched Stewart [11] hysteresis Ruaumoko model loops for Wall W5 is shown in Figure 27.

Wall W7 was the same construction as Wall W6 but the specimen was tested after the test regime on WallSetD (See Section 10) – i.e. the wall was initially in a softened state due to pre-testing. The Ruaumoko model was fitted to the measured hysteresis loops as shown in Figure 28.

Three 2DOF constructions were tested as separated two-storey walls as illustrated in Figure 1(b) and Figure 6(a). These are summarised in Table 4. WallSetA was designed to try to force a semblance of base isolation (i.e. the top storey was expected to be only slightly damaged). WallSetB was designed to try to achieve a balanced failure – i.e. similar damage in both walls.

Table 4: Two-storey Walls PD-Tested as Separated Walls

Name	Top Wall	Bottom Wall	M1 (Tonnes)	M2 (Tonnes)	T1 (Seconds)	T2 (Seconds)
WallSet A	Wall6	Wall6	2.4	2.4	0.4075	0.1556
WallSet B	Wall5	Wall6	2.1	2.1	0.3840	0.1484
WallSet B*	Wall5	Wall6	3.0	2.2	0.4125	0.1690
WallSet C	Wall5	Wall7	3.0	2.2	0.4125	0.1690

* Used for 1.2 El Centro earthquake only

9.2 Results

All the PD tests and ITHA used 5% damping. The PD runs used the same initial stiffnesses used in the Ruaumoko analyses and the assumed building periods as given in Table 4 were as computed from the Ruaumoko analyses. Thus, the damping coefficients defined in Section 7.2 were the same for both PD and Ruaumoko analyses.

A comparison of the deflections measured in the PD test and that determined from the ITHA are given in the figures listed in Table 5. This table also shows the testing program imposed on each wall. The ITHA simulated the whole time history of loading but the comparison is only presented for the final loading.

9.3 Sensitivity Analysis

The assumed shape of the hysteresis loops can significantly affect the deflections computed by ITHA. This is illustrated in Figure 33 which is a plot of the deflection time history of the ITHA for 1.0 El Centro excitation of the two-storey structure with Wall W1 being assumed at the upper level and either Wall W4, W6 or W7 being assumed at the lower level. The difference between Wall W4, W6 and W7 hysteresis loops is not

great but clearly has lead to a significant difference in deflections, particularly at Level 1. This indicates a sensitivity in the degree of base isolation. When comparing Figure 33 with the preceding 2DOF deflection time history plots it can be seen that the degree of agreement obtained between ITHA simulation and PD test was good, indicating good agreement between modelled hysteresis loops and the actual performance of the test specimen.

9.4 Conclusions from ITHA and PD Tests

Generally a very good agreement was obtained between the ITHA and the PD test deflections. This deteriorated at large deflections and was best at mid-range deflections. The seismic deflections in a 2DOF structure are sensitive to the degree of base isolation – i.e. the relative strength/stiffness of the upper and lower floors.

Table 5: Comparison of Deflections Measured in PD Testing and Ruaumoko Simulation of 2DOF Walls

WallSet Type	Figure No For Cyclic Testing	Figure No For PD and Ruaumoko Comparison	Factor Used on El Centro Earthquake
A	Figure 26	–	0.5
A		Figure 29	1.0
A		Figure 30	1.5
B	Figure 26-27	–	0.5
B		Figure 31	1.0
B	*	–	1.2
E	Figure 27-28	Figure 32	1.0

* Used a different mass distribution – see Table 3

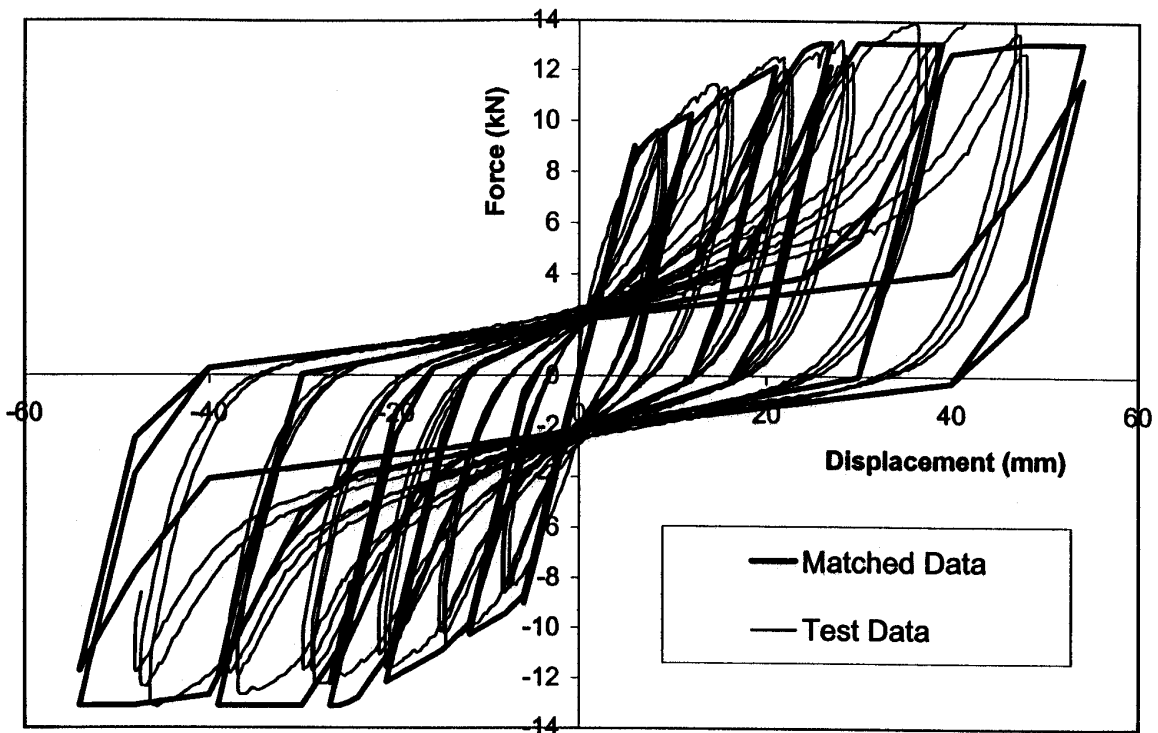


Figure 26: Wall W6. Cyclic Test and Ruaumoko Modelled Hysteresis Loops

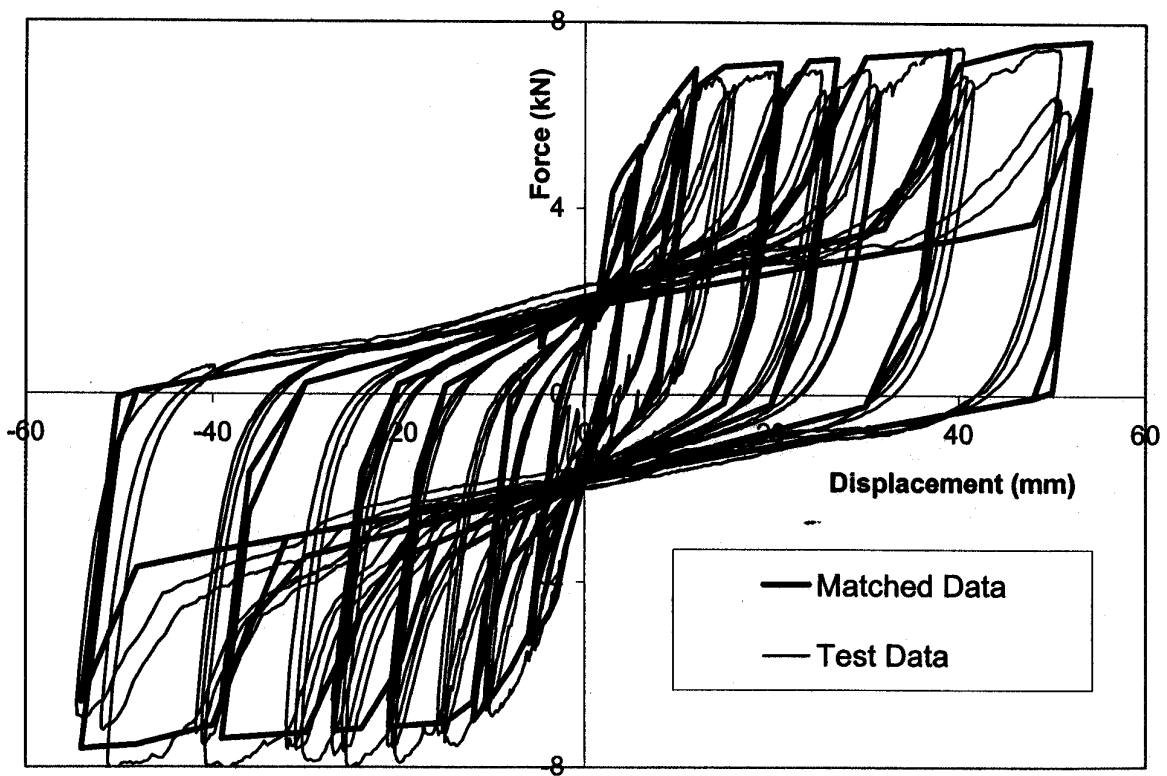


Figure 27: Wall W5. Cyclic Test and Ruaumoko Modelled Hysteresis Loops

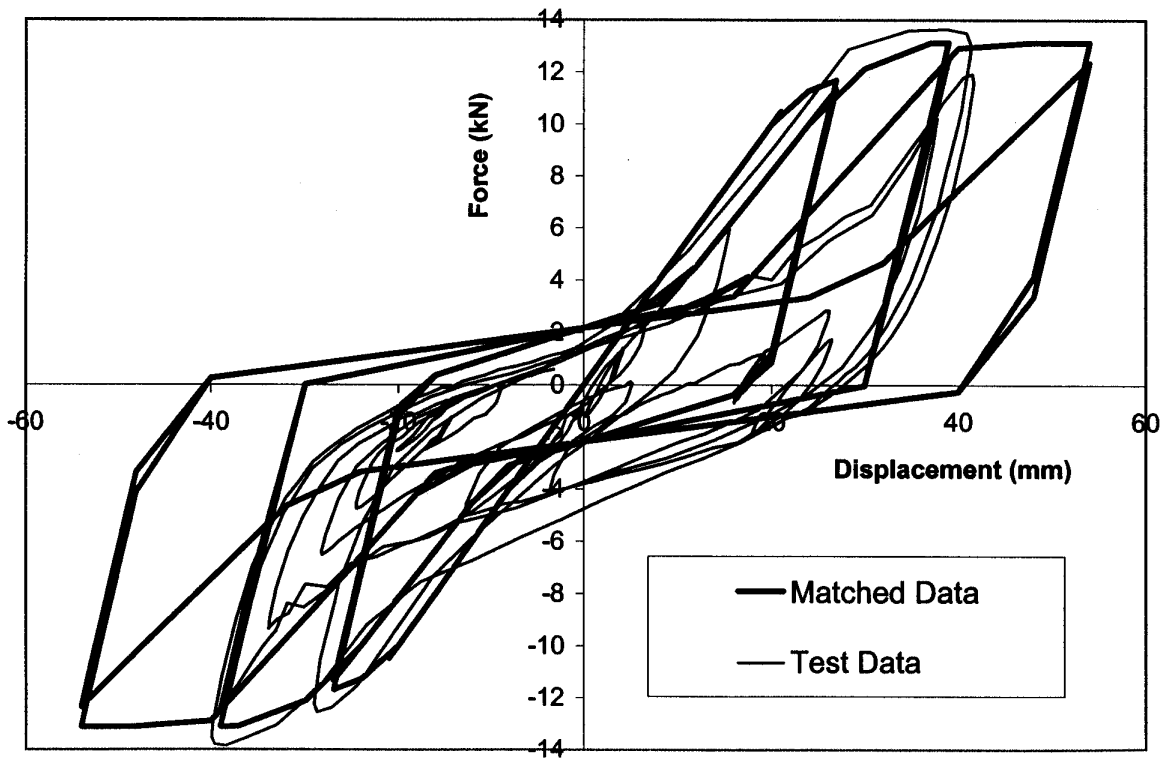
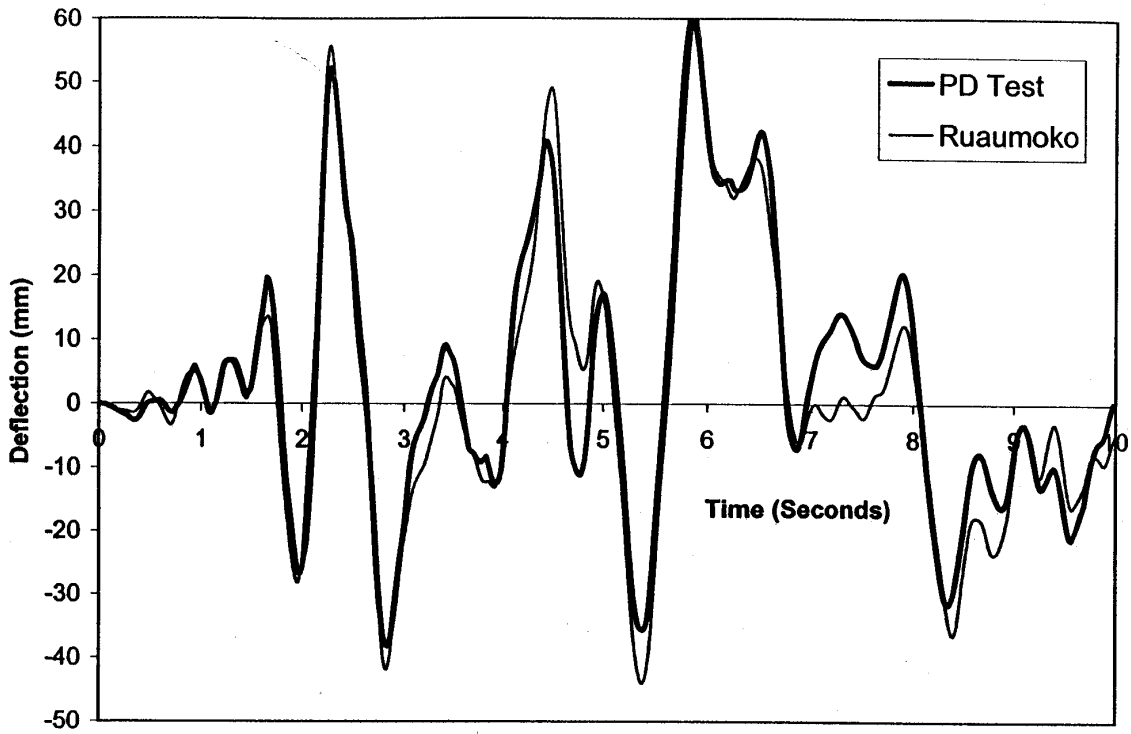
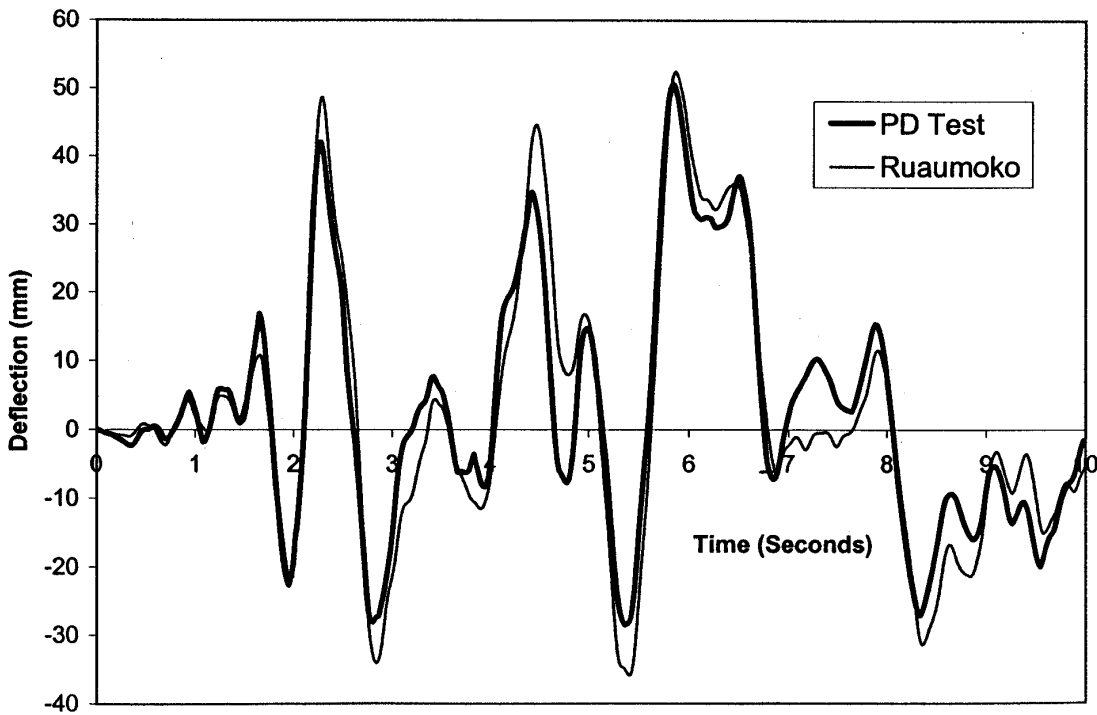


Figure 28: Wall W7. PD Test and Ruaumoko Modelled Hysteresis Loops

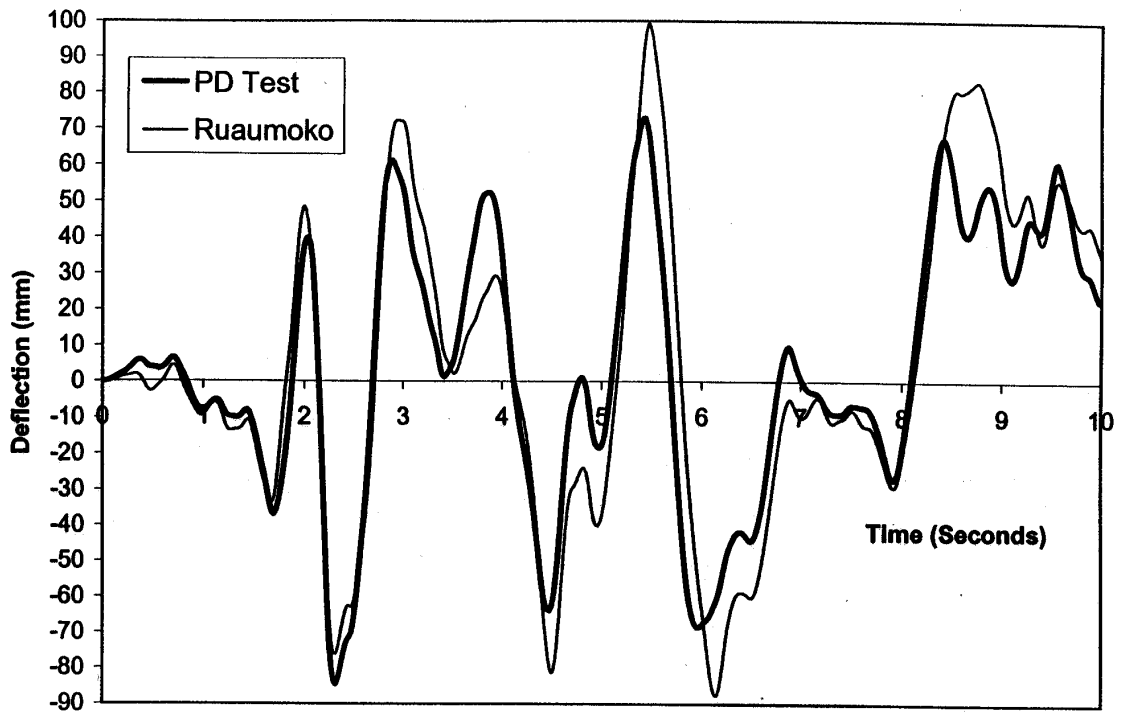


(a) Level 2 Deflections

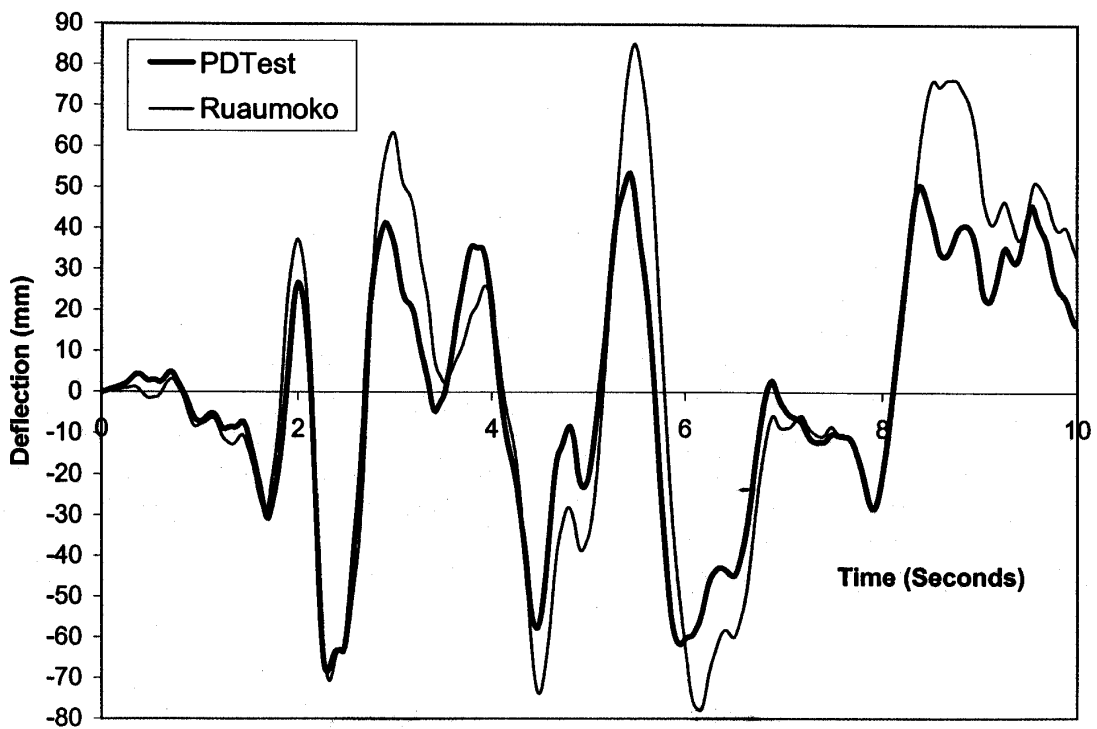


(b) Level 1 Deflections

Figure 29: Comparison Ruaumoko and PD. WallSet A, 1.0 El Centro EQ

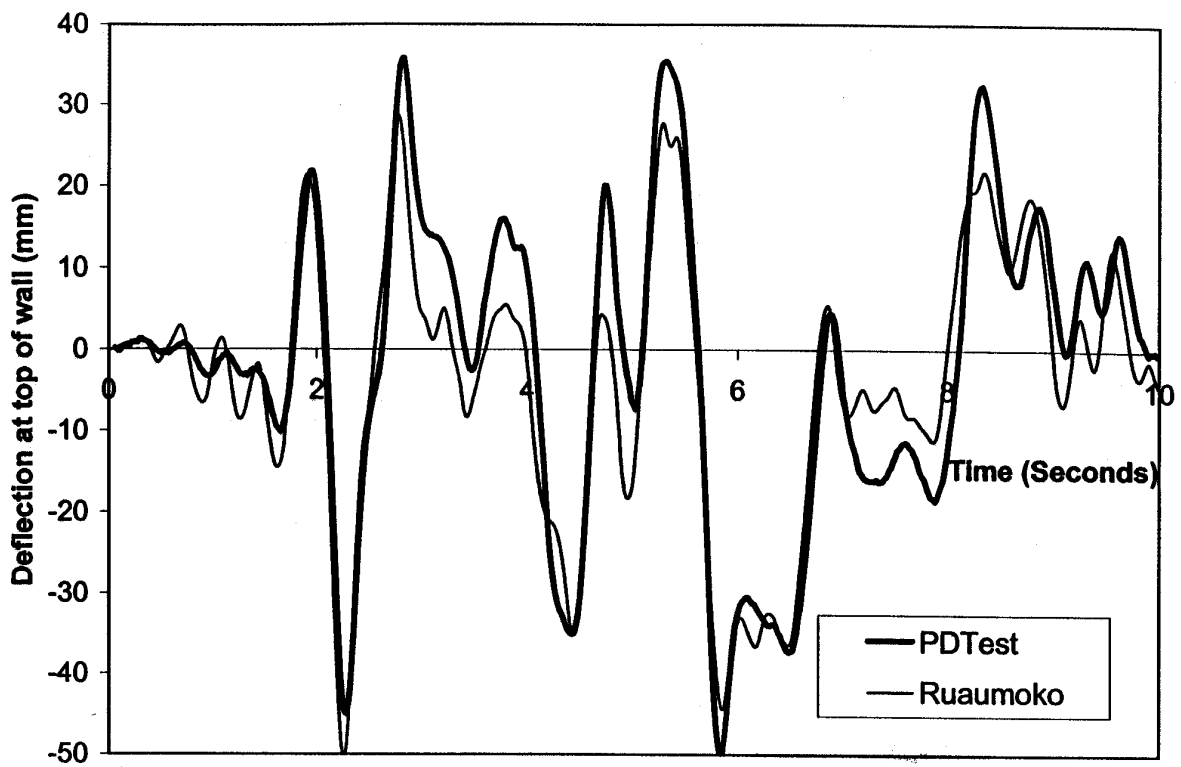


(a) Level 2 Deflections

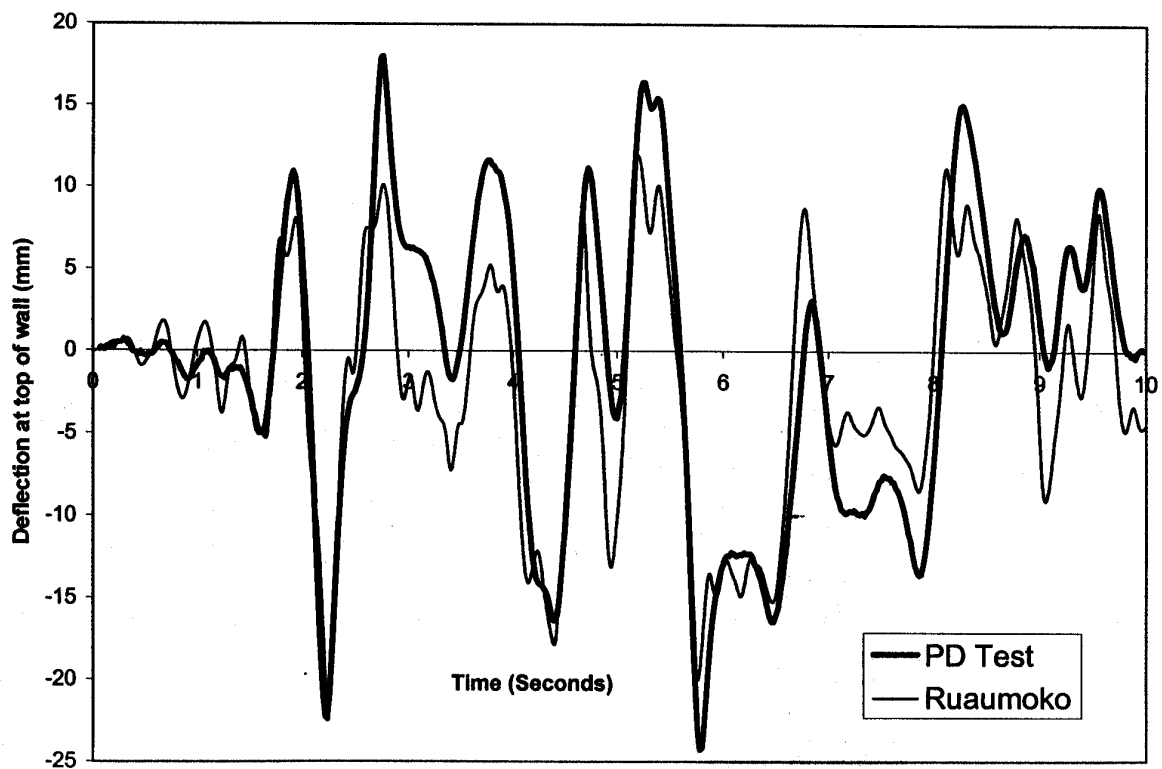


(b) Level 1 Deflections

Figure 30: Comparison Ruaumoko and PD. WallSet A, 1.5 El Centro EQ

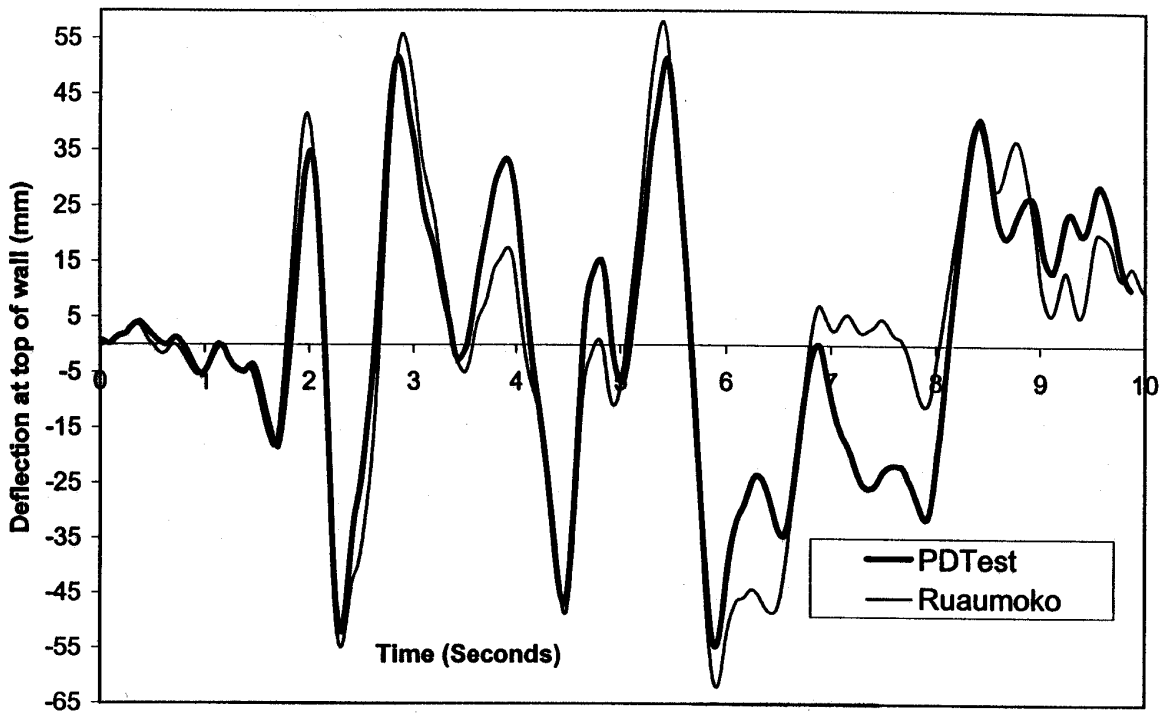


(a) Level 2 Deflections

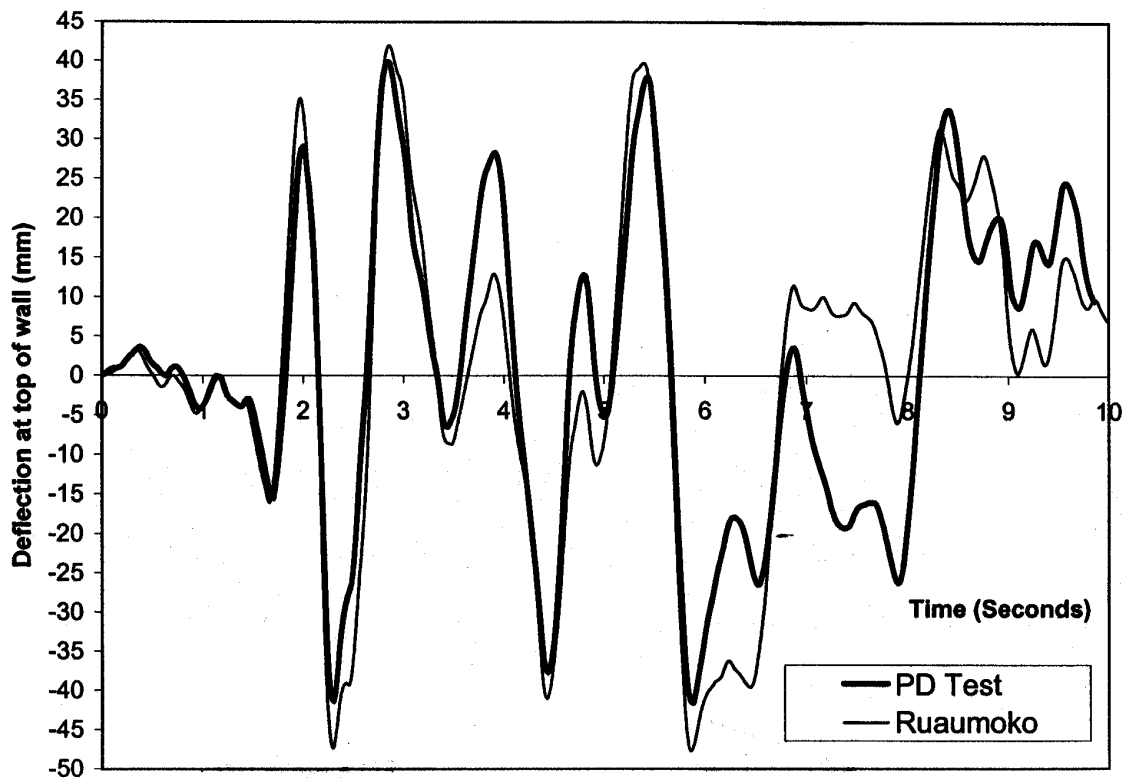


(b) Level 1 Deflections

Figure 31: Comparison Ruaumoko and PD. WallSet B, 1.0 El Centro EQ

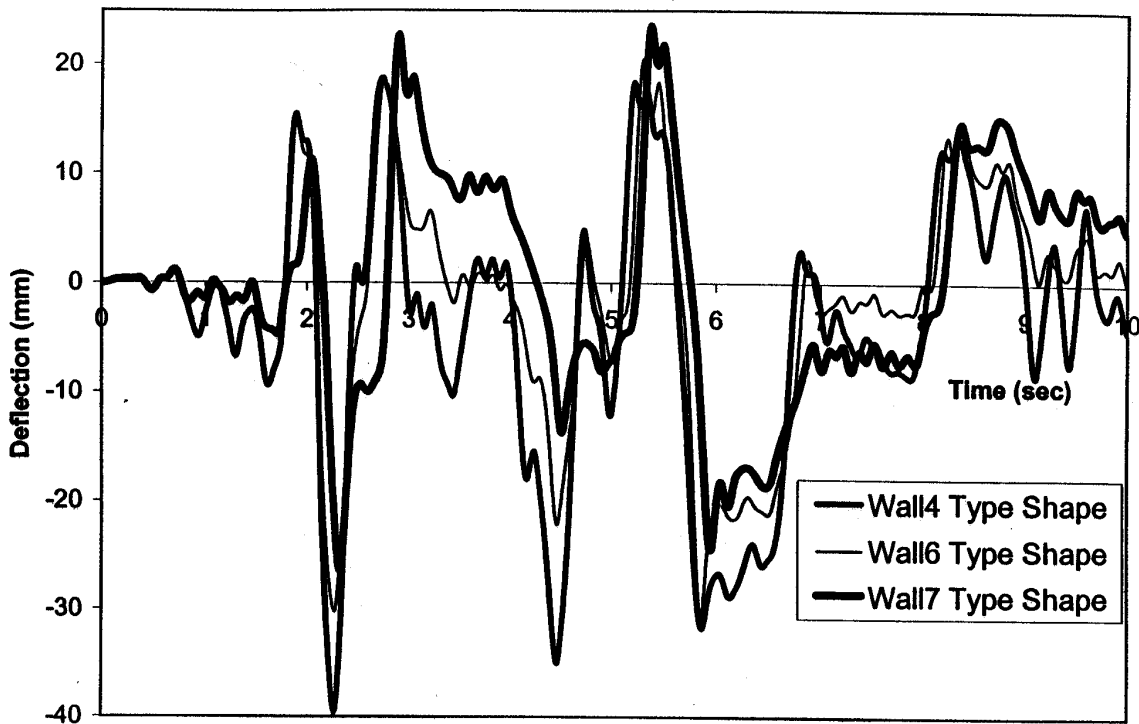


(a) Level 2 Deflections

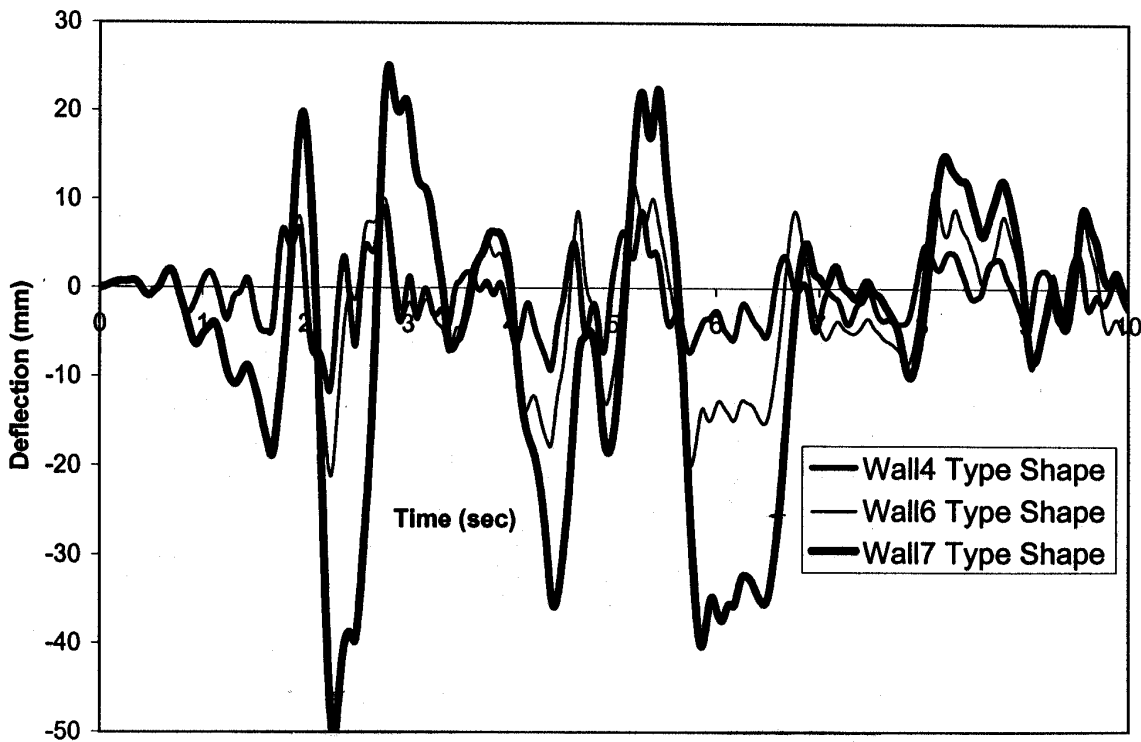


(b) Level 1 Deflections

Figure 32: Comparison Ruaumoko and PD. WallSet E, 1.0 El Centro EQ

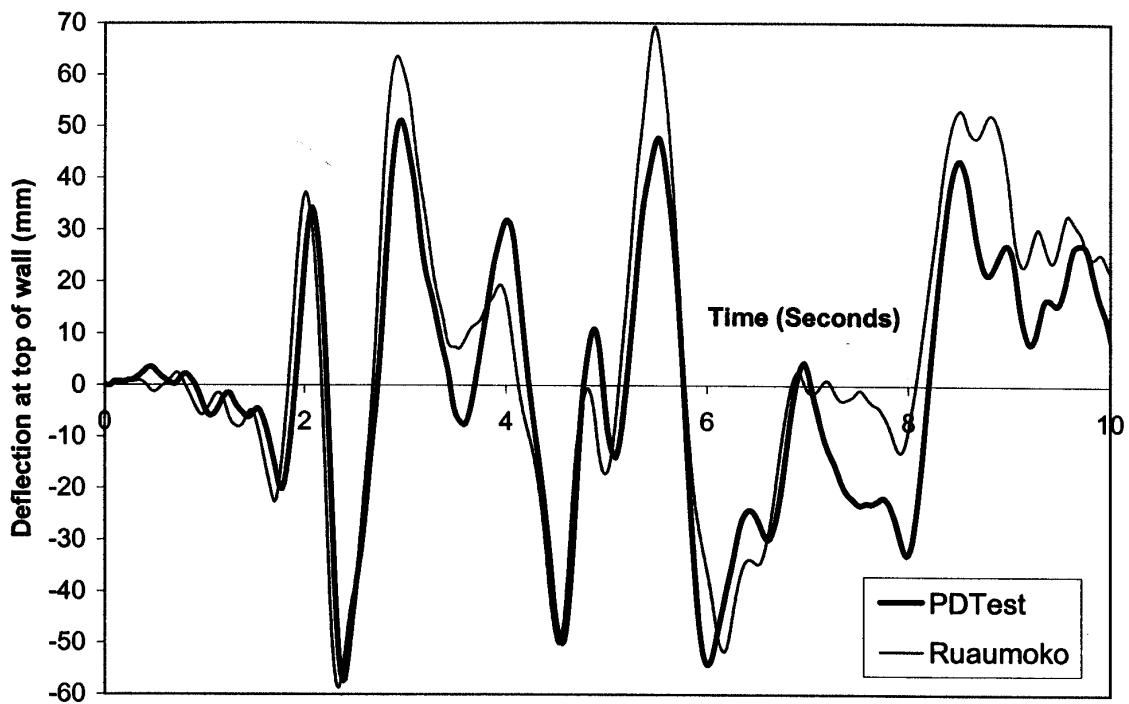


(a) Level 2 Deflections

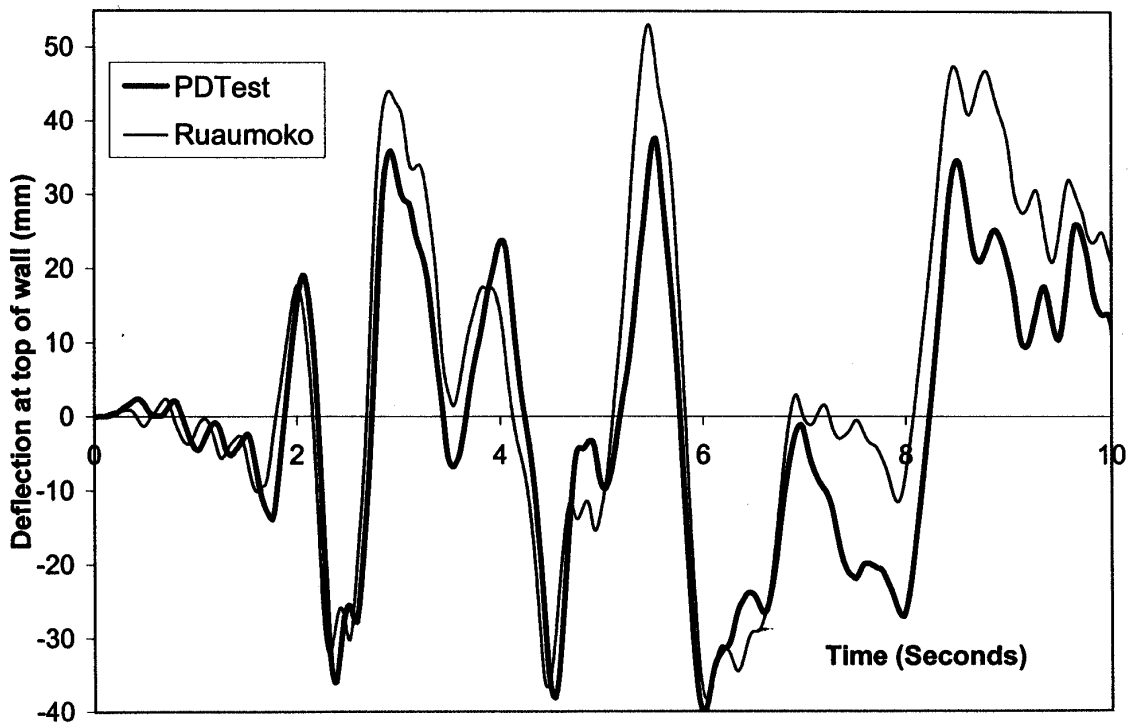


(b) Level 1 Deflections

Figure 33: Sensitivity Analysis WallSet B, 1.0 El Centro EQ

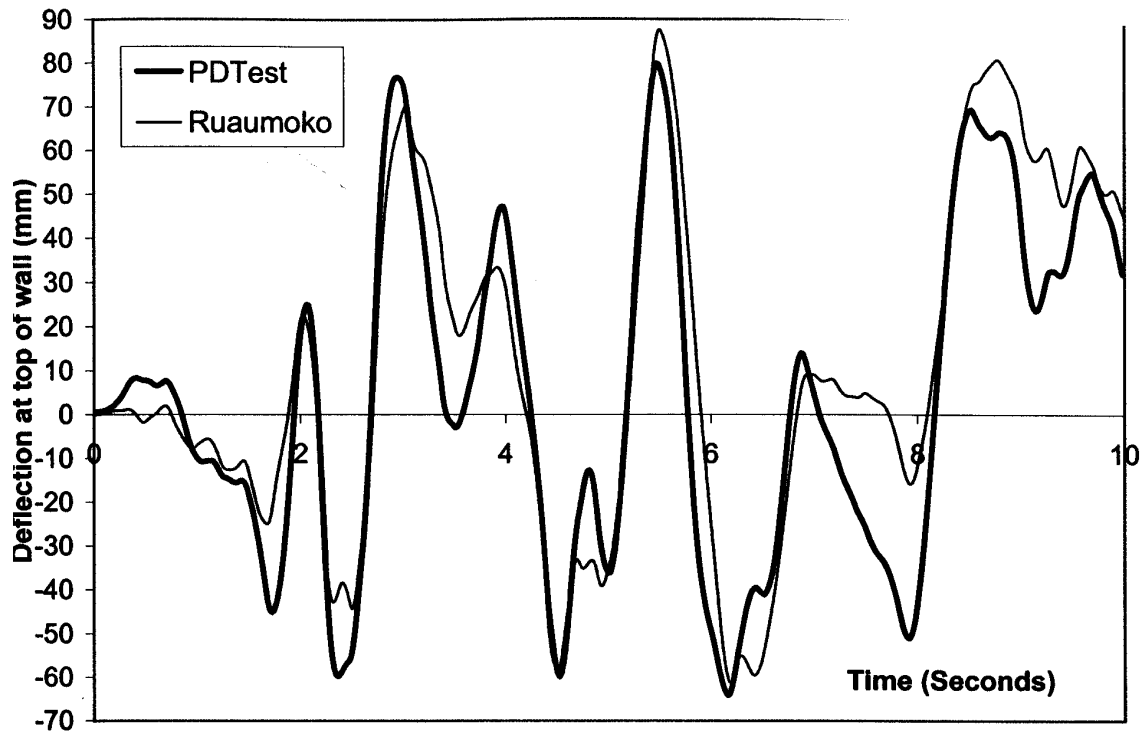


(a) Wall Type 5 Deflections

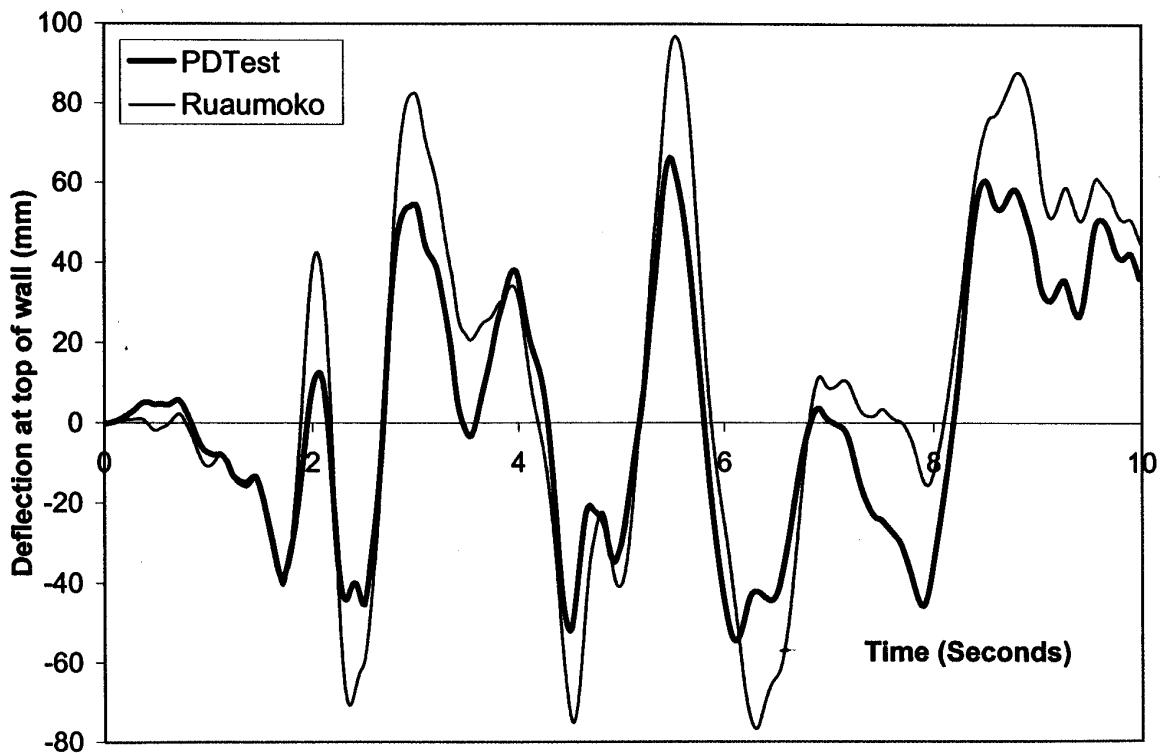


(b) Wall Type 7 Deflections

Figure 34: Comparison Ruaumoko and PD. WallSet C, 1.0 El Centro EQ

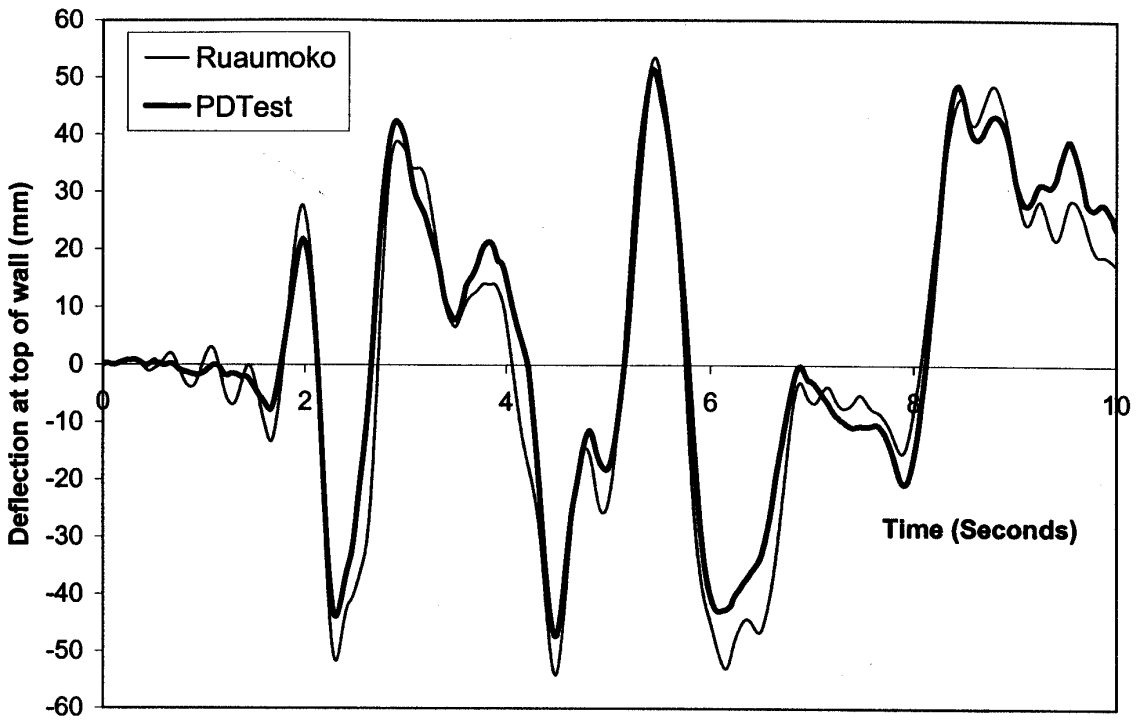


(a) Wall Type 5 Deflections

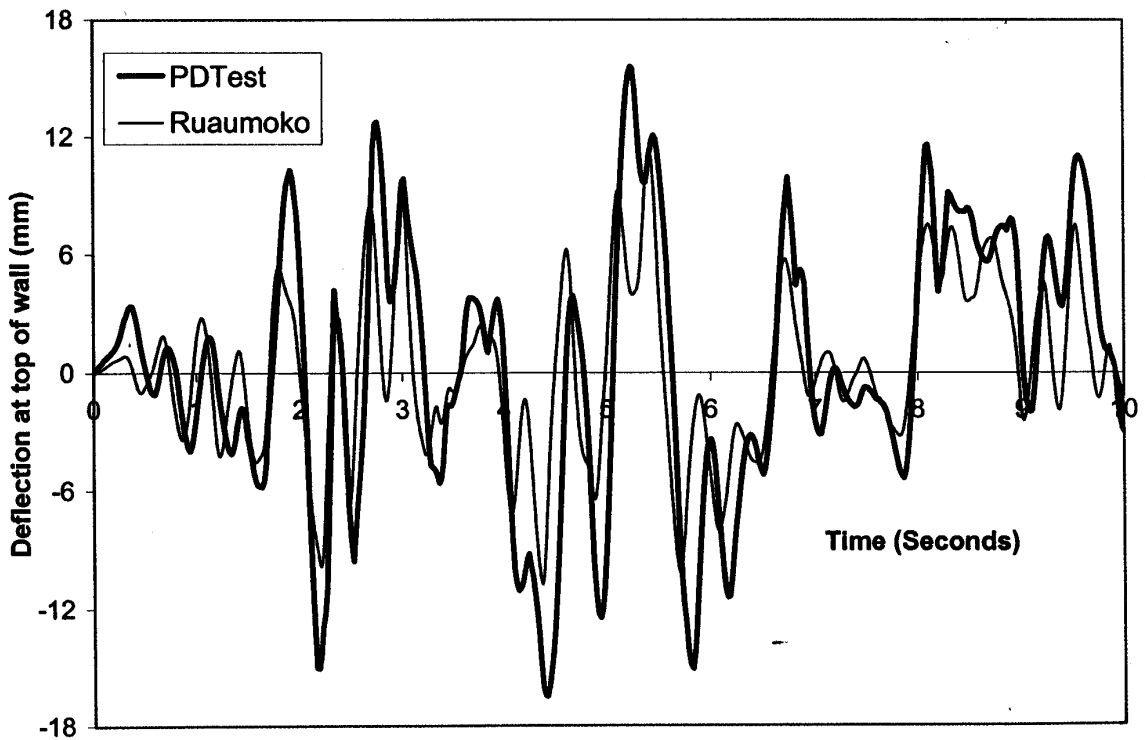


(b) Wall Type 7 Deflections

Figure 35: Comparison Ruaumoko and PD. WallSet C, 1.3 El Centro EQ



(a) Wall Type 5 Deflections



(b) Wall Type 7 Deflections

Figure 36: Comparison Ruaumoko and PD. WallSet D, 1.0 El Centro EQ

10. VERIFICATION OF PROGRAM BY TORSION TESTS

10.1 Construction

The tests in this series used Walls W5 and W7 as defined in Table 1. These were tested as a single-storey configuration as detailed for the two types of torsion models considered in this report and as defined in Sections 7.4 and 7.5. The configurations are referred to as WallSet C and WallSet D respectively. The following assumptions were made:

Wallset C. The system assumed is illustrated in Figure 1(c) with the earthquake being in the X direction and $D1=D2=6$ m; $D = 12$ m. Walls W1 and W2 (see Figure 1(c)) were constructed as per Walls W5 and W7 respectively. Wall W3 and W4 as depicted in Figure 1(c) were both assumed to be purely elastic of stiffness 500 kN/m with $D = 2$ m. Building mass $M = 10$ tonnes.

Wallset D. The system assumed is illustrated in Figure 1(c) with the earthquake being in the EQ2 direction (i.e. at 45° to the main axes). Walls W1 and W2 (see Figure 1(c)) were constructed as per Walls W5 and W7 respectively. Walls W3 and W4 (see Figure 1(c)) were assumed to be identical to Walls W1 and W2 respectively. Building mass $M = 12$ tonnes.

10.2 Results

All the PD tests and ITHA used 5% damping. The mass distribution used in the Ruaumoko analyses was selected to provide the same rotational moment of inertia as used in the PD and Excel analyses as described in Section 7.4.

A comparison of the deflections measured in the PD test and that determined from the Ruaumoko simulation are given in the Figures listed in Table 5. This table also shows the testing program imposed on each wall. The ITHA simulated the whole time history of loading but the comparison is only presented for the final loading.

10.3 Conclusions

Generally a very good agreement was obtained between the ITHA and the PD-test deflections and the results illustrated that significant twist may occur in a house with strong stiff walls on two sides and weaker walls on the other two sides.

Table 6: Comparison of Deflections Measured in PD Testing and Ruaumoko Simulation of Torsion Configuration Walls

WallSetType	Figure No. for PD and Ruaumoko Comparison	Factor Used on El Centro Earthquake
C	-	0.5
C	Figure 34	1.0
C	Figure 35	1.3
D	Figure 36	1.0

11. COMPARISON OF RUAUMOKO, EXCEL AND PD THEORETICAL ANALYSES

A theoretical analysis was performed on the structures summarised in Table 7 under excitation from the modified El Centro earthquake. Analyses were done for both purely elastic and bilinear hysteresis elements. A sketch of the structures analysed is shown in Figure 1.

Details of the modified El Centro earthquake used are given in Appendix A. The earthquake for Structures 5 and 6 was assumed to be parallel to X axis. The earthquake for Structure 7 was assumed to be at 45° to the main axes in the direction shown as EQ2 in Figure 1.

Structures 1-7 were analysed by each of Ruaumoko, Excel spreadsheet and theoretical PD software. To avoid this report becoming excessively large, plots of the results are not given herein but are available from the writer on request. In all instances there was close to a precise agreement in all corresponding Ruaumoko, Excel spreadsheet and theoretical PD analyses which provides confidence in the programming. The differences were indistinguishable when data was plotted.

It is interesting to note that the maximum deflection in Structure 6 was only 7% greater than in Structure 5 (although it occurred at a later time) even though the yield stiffnesses of Wall W1 and Wall W2 were only 5% of the initial stiffness. This was because the perpendicular walls were relatively stiffer than the parallel walls (in their post yield condition) and thus reduced the diaphragm rotation.

Large diaphragm rotations occurred in the Structure 7 analyses. The weaker walls in both directions had large yield deformations but the stiffer walls did not yield and exhibited very small deflections. However, the maximum deflection of the weaker walls was 14% smaller than in Structure 5 which was not an expected result. This indicates that the response of houses under bi-axial earthquakes where weaker walls in both directions are yielding is unlikely to be significantly greater than from a uni-axial earthquake.

Table 7: Summary of Structures Analysed

Struct. No.	K1 (kN/m)	K2 (kN/m)	R (%)	Fy1 (kN)	Fy2 (kN)	M1 (kg)	M2 (kg)	Type	K (kN/m)
1	800	-	-	-	-	6000	-	Elastic	-
2	800	500	-	-	-	3000	3000	Elastic	-
3	800	-	10	10	-	6000	-	Bilinear	-
4	800	500	10	10	6	3000	3000	Bilinear	-
5	5500	1700	-	-	-	30500	-	Elastic	3600
6	5500	1700	5	55	17	30500	-	Bilinear	3600
7	5500	1700	5	55	17	30500	-	Bilinear	*

* Properties of Wall W3 and Wall W4 were made identical to Wall W1 and Wall W2 respectively.

12. CONCLUSIONS

For single-storey and two-storey timber-framed sheathed shear walls, the pseudo-dynamic (PD) test method has been shown to give very good agreement with seismic simulation by inelastic time history analysis (ITHA). The ITHA used the Ruaumoko software package. Care needs to be taken to ensure that the Ruaumoko modelled hysteresis loops truly reflect specimen performance. A good agreement was also found for single-storey torsion simulation. It was concluded that the PD test method was likely to be better than the computer simulation because it reflected actual specimen performance, including non-symmetry, and was likely to better predict drift to one side. Due to modelling constraints with the Stewart [11] element used it is likely that the ITHA will be most in error at smaller displacements where the wall first starts to show significant non-linearity, and at large displacements where the tri-linear backbone curve used becomes inaccurate.

Agreement has been shown by others between shake and computer analysis and in one instance by computer analysis and PD test. Good agreement between computer analysis and PD test has been found in this project. Therefore, for the structures considered in this project, it is believed that the pseudo-dynamic (PD) test method has been proven.

13. REFERENCES

1. Takanashi, K. et al. 1974. Seismic failure analysis of structures by computer pulsator on-line system. *Journal of the Institute of Industrial science, University of Tokyo.* 26(11): 13-25.
2. National Instruments Corporation, 2000. LabView Version 6 software.
3. Carr A.J., Ruamoko. 2000. Computer Program User Manual. University of Canterbury, New Zealand.
4. Thurston S.J. and Park S.G., 2002 Seismic Design of New Zealand Houses. Paper submitted to NZNSEE.
5. Standards New Zealand 1999. Timber Framed Buildings. NZS 3604, Wellington, New Zealand.
6. Mahin, S.A., Shing, P.B. 1985. Pseudo-Dynamic method for seismic testing. *Journal of Structural Engineering* 111(7):1482-1503.
7. Seible, F.; Hegemier, G.A.; Priestley, M.J.N. 1991. Full-scale testing of structural masonry systems under simulated seismic loads. In: *Proceedings, Pacific Conference on Earthquake Engineering*, 20-23 November, Auckland, New Zealand. 2:197-208.
8. Kamiya, Fumio. 1988. Nonlinear earthquake response analysis of sheathed work walls by computer-actuator on-line system. *Proceedings, 1988 International Conference on Earthquake Engineering*; Sept 19-22; Seattle, Washington. 838-847.
9. Ceccotti A., Follesa, M. and Daracabeyli. 2000. E., 3D seismic analysis of multi-storey wood frame construction. WCTE 2000. *World Conference on Timber engineering*, Whistler, BC, Canada. August 2000.
10. Fischer, D., Filiatrault, A, Folz, B, Uang, C-M and Seible, F. 2000. Shake-table Tests of a Two-Storey House. *Structural Systems Research Report No. SSRP 2000/15.*

11. Stewart, W.G., Dean, J.A. and Carr, A.J. 1988. The earthquake behaviour of plywood sheathed shear walls, Proc 1988 International Conference on Timber Engineering, Seattle, Washington. pp. 248-261.
12. Folz, B. and Filiatrault, A. 2000. Cashew – Version 1.0. A computer program for cyclic analysis of wood shear walls. Structural Systems Research Report No. SSRP 2000/10, Department of Structural Engineering, University of California, San Diego.
13. Deam, B.L. and King, A.B. 1996. Pseudo-dynamic seismic testing of structural timber elements. Proceedings, International Wood Engineering Conference, New Orleans, Louisiana, 1:53-59.
14. Yamaguchi, N. and Minowa, C. 1998. Dynamic performance of Wooden Bearing Walls By Shaking Table Test. Proc. Fifth World Conference on Timber Engineering. August 17-20, 1998, Montreux, Switzerland. V2, pp 26-334.
15. Kohara, K. and Miyazawa, K. 1998. Full-Scale Shaking Test of Two-storey Wooden Dwelling Houses. Proc. Fifth World Conference on Timber Engineering. August 17-20, 1998, Montreux, Switzerland. V2, pp 548-555.
16. Chopra Anil K. Dynamics of Structures, 2000. Theory and Application to Earthquake Engineering. Second Edition. Prentice Hall. New Jersey, 844 pages.
17. Standards New Zealand 1992. General Structural Design and Design Loadings For Buildings. NZS 4203. Wellington, New Zealand.
18. Cooney, R.C. and Collins, M.J. 1979 (revised 1982, 1987, 1988, 1990). A wall bracing test and evaluation procedure. BRANZ Technical Paper P21. Judgeford, New Zealand.

14. ACKNOWLEDGEMENTS

The author acknowledges financial support for this project from the Building Research Levy and Carter Holt Harvey for supply of timber used in this programme.

Appendix A: Modified El Centro Earthquake

The Modified El Centro earthquake was produced by Dr Barry Davidson of the University of Auckland by modification of the 1940 NS El Centro earthquake to fit the NZS 4203 [17] earthquake as shown in Figure 37. A time history of the earthquake motion is given in Figure 38. Only the first 10 seconds of this earthquake were used in the PD runs.

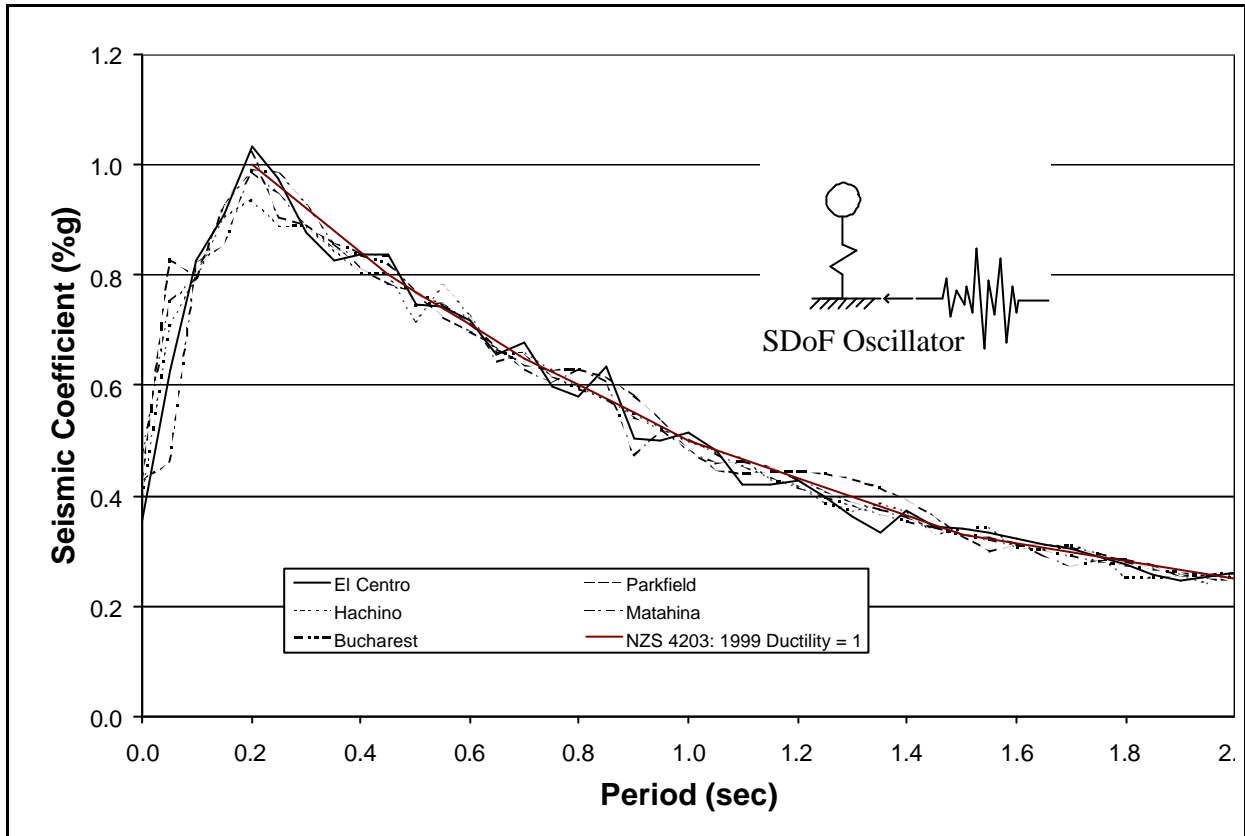


Figure 37: Comparison of the NZS4203 [17] and Modified El Centro response spectrum

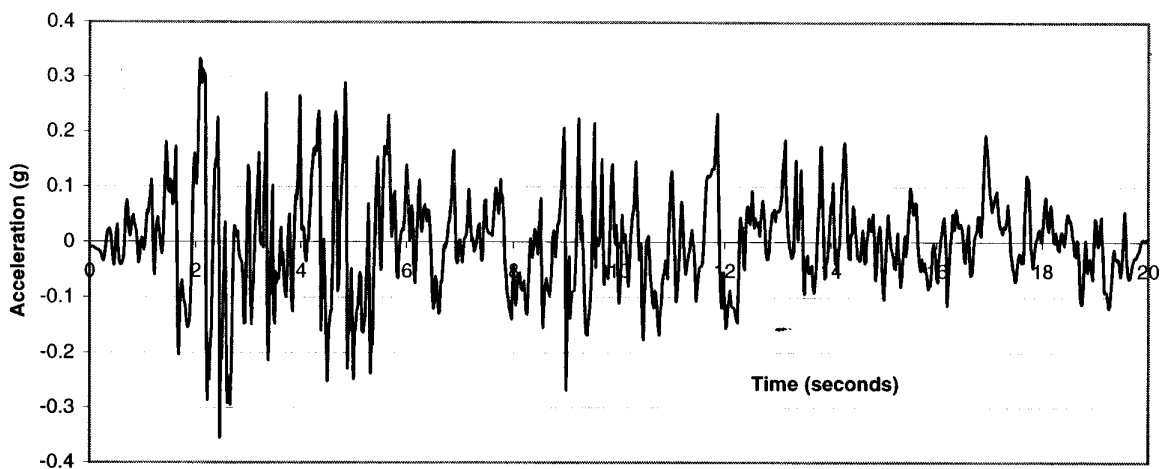


Figure 38: Modified El Centro Earthquake Acceleration Record